Fly palaeo-evo-devo: Immature stages of bibionomorphan dipterans in Baltic and Bitterfeld amber

Viktor A Baranov [Corresp., 1], **Mario Schädel** [1], **Joachim T Haug** [1, 2]

[1] Biology II, Ludwig-Maximilians-Universität München, Planegg, Bayern, Германия

[2] Geobio-Center, Ludwig-Maximilians-Universität München, Planegg, Bayern, Германия

Corresponding Author: Viktor A Baranov
Email address: baranow@biologie.uni-muenchen.de

Larvae of flies and gnats (Diptera) form a crucial component of many terrestrial and freshwater ecosystems in the extant biosphere. Larvae of Diptera are playing central role in water purification, matter and energy transfer in riparian ecosystems in rivers, carbon cycling in lakes and forests as well as being major destructors of the dead organic matter. Despite all these important roles, dipteran larvae are most often ignored in palaeoecological studies, due to the difficulty of the taxonomic identification of fossil larva, but also, due to the perceived importance of adult dipterans in palaeoentomological and taxonomic studies. Despite that, much information on palaeoecosystems can be gained from studying fossil dipteran larvae, in particular for well preserved specimens from fossil resins (ambers and copals). Since ambers are selectively preserving fauna of trunks and leaf litter, it allows us to learn a lot about xylophages and saprophages of amber forests, such as Eocene Baltic amber forest. Here we present immature stages (larvae and pupa) of the dipteran ingroup Bibionomorpha, from Baltic and Bitterfeld Amber forests. We have recorded at least four different larval morphotypes, one with four distinct instars, and at least three pupal morphotypes. One larva is recognised as a new species, either a highly derived ingroup of Bibionidae or sister species to it. Also represented by single larval specimens are the groups Pachyneura (Pachyneuridae) and Sylvicola (Anisopodidae). The majority of the recorded specimens are representatives of the group Mycetobia (Anisopodidae). Due to abundance of Mycetobia immature stages, we have been able to reconstruct the number of larval stages and growth rate of these fossil Diptera. We discuss implications of these finds.

Fly palaeo-evo-devo: Immature stages of bibionomorphan dipterans in Baltic and Bitterfeld amber

Viktor Baranov[1], Mario Schädel[1], Joachim T. Haug[1, 2]

[1] Department of Biology II, LMU Munich, Großhaderner Str. 2, 82152, Martinsried-Planegg, Germany

[2] GeoBio-Center, LMU Munich, Großhaderner Str. 2, 82152, Martinsried-Planegg, Germany

Corresponding Author:
Viktor Baranov[1]
Department of Biology II, LMU Munich, Großhaderner Str. 2, 82152, Martinsried-Planegg, Germany.
Email address: baranow@biologie.uni-muenchen.de

Abstract

Larvae of flies and gnats (Diptera) form a crucial component of many terrestrial and freshwater ecosystems in the extant biosphere. Larvae of Diptera are playing central role in water purification, matter and energy transfer in riparian ecosystems in rivers, carbon cycling in lakes and forests as well as being major destructors of the dead organic matter. Despite all these important roles, dipteran larvae are most often ignored in palaeoecological studies, due to the difficulty of the taxonomic identification of fossil larva, but also, due to the perceived importance of adult dipterans in palaeoentomological and taxonomic studies. Despite that, much information on palaeoecosystems can be gained from studying fossil dipteran larvae, in particular for well preserved specimens from fossil resins (ambers and copals). Since ambers are selectively preserving fauna of trunks and leaf litter, it allows us to learn a lot about xylophages and saprophages of amber forests, such as Eocene Baltic amber forest. Here we present immature stages (larvae and pupa) of the dipteran ingroup Bibionomorpha, from Baltic and Bitterfeld Amber forests. We have recorded at least four different larval morphotypes, one with four distinct instars, and at least three pupal morphotypes. One larva is recognised as a new species, either a highly derived ingroup of Bibionidae or sister species to it. Also represented by single larval specimens are the groups Pachyneura (Pachyneuridae) and Sylvicola (Anisopodidae). The majority of the recorded specimens are representatives of the group Mycetobia (Anisopodidae). Due to abundance of Mycetobia immature stages, we have been able to reconstruct the number of larval stages and growth rate of these fossil Diptera. We discuss implications of these finds.

Introduction

Holometabola is a hyperdiverse group of organisms, representing the dominant part of animal life in terrestrial ecosystems (Grimaldi & Engel, 2005). Representatives of the group such as bees, butterflies, beetles and mosquitoes are therefore to most people the best known forms of Insecta. The dominance of holometabloans has led researchers to consider Holometabola as one of the most successful groups of Metazoa (Grimaldi & Engel, 2005, Engel, 2019). The evolution of niche differentiation between the larva (see Haug, in press) and the adult has been interpreted as one of the driving factors of their success. The evolutionary independence of different life stages and phases (see Scholtz, 2005) has allowed holometabolans to utilize a very wide spectrum of habitats and ecological niches (Grimaldi & Engel, 2005).

Larvae of flies and midges (representatives of the group Diptera) are particularly successful in diverse habitats, from glaciers at the Antarctic mainland to the fast-drying rock pools of central Africa (Marshall, 2012; Armitage et al., 1995). Due to such variety of habitats occupied, larvae of Diptera have become involved in numerous critical ecosystem functions (Marshall, 2012). Dipteran larvae are crucial saprophages, destroying dead organic matter in both aquatic and terrestrial ecosystems, and therefore are driving biogeochemical cycles of matter and energy, in riparian ecosystems in rivers (Marshall, 2012; McAlister, 2017). This ecological role of larval forms of Diptera became especially important about 80 million years ago, in the Upper Cretaceous, when due to the Cretaceous Terrestrial Revolution (CTR) angiosperm plants have become prominent players in the ecosystem (Fastovsky et al., 2004; Mckenna et al., 2015).

The emergence of angiosperm plants in terrestrial ecosystem has led to an increased load of dead organic matter into the terrestrial and freshwater ecosystem (Kalugina, 1974a, b; Mckenna et al., 2015). Such a drastic ecosystem change has led to shifts in the communities of various lineages of Insecta (Kalugina, 1974a, b). Such shifts included the extinction or diminishing of certain systematic and ecological groups. Among them were nectic and benthic oxyphilic forms living in “dystrophic” lakes. Vice versa, other groups, such as specialized pollinators or saprophages, have experienced an enormous diversification (Sinichenkova & Zherikhin, 1996). Among the groups experiencing a pronounced diversification were many ingroups of Diptera (Grimaldi & Engel, 2005). Numerous groups of dipterans with terrestrial larvae are associated with decaying organic material, such as dead wood, fungal fruit bodies, dead leaves, or animals corpses (Keilin & Tate, 1940; Marshall, 2012). Among the most abundant extant saprophagous forms of Diptera (with predominantly terrestrial larvae) are representatives of Bibionomorpha (Marshall, 2012; Ševčík et al., 2016).

The monophyly of the group has been rarely questioned, yet the exact relationships of its ingroups are reconstructed differently from author to author (Skartveit & Willasen, 1996; Ševčík et al., 2016). Many authors interpret Bibionomorpha as the sister group to Brachycera, forming the supposedly monophyletic group Neodiptera (Ševčík et al., 2016). Bibionomorpha includes numerous ecologically similar ingroups (Fig. 1, modified from Ševčík et al., 2016).

The geological history of the Bibionomorpha spans more than 220 million years (Blagoderov et al., 2007). Many representatives are known from the late Triassic (Blagoderov et al., 2007) and Jurassic (Kalugina and Kovalev, 1985). Despite the long evolutionary history of the group and the ecological importance of their larval stages, very little attention has been paid to the fossil records of immature stages of Bibionomorpha (Harris, 1983; Skartveit, 2008). This is surprising, as immature representatives of Bibionomorpha, especially those of Anisopodidae, seem quite common in amber (as we will demonstrate). Despite such abundance, Anisopodidae larvae from amber were only mentioned in a single study focused on specimens from Dominican amber (Grimaldi, 1991).

Here, we present a first overview of the immature stages of Bibionomorphan from amber, including larvae and pupae of Anisopodidae, larvae of Pachyneuridae and a species that seems closely related to Bibionidae. All specimens in focus of this study are preserved in Eocene Bitterfeld amber and Baltic ambers (Table 1). We also discuss the implications of the phylogenetic and ecological diversity of immature representatives of Bibionomorpha for our understanding of the ecology and biogeochemistry of the Eocene amber forests.

Materials & Methods

Material

All specimens, in total 56, in the center of this study are preserved in amber and come from various collections.

Part of the material (see table 1, material marked as “Material from Hoffeins collection”) was obtained commercially in 2005 and stems from Yantarnyj, Kaliningrad district (formerly Palmnicken, Königsberg); specimens have temporarily been part of the collection of Christel and Hans-Werner Hoffeins (CCHH). All specimens from this source are now deposited at the Senckenberg Deutsches Entomologisches Institut (SDEI) with the inventory numbers (listed in table 1). Another part of the material comes from the private collection of Carsten Gröhn and is now deposited in the collection of the Center for Natural History in Hamburg (Centrum für Naturkunde, CeNak), formerly Geological-Paleontological Institute and Museum of the University of Hamburg (Geologisch-Paläontologisches Institut und Museum der Universität Hamburg, GPIH).

Part of the material was obtained commercially from Jonas Damzen (“amberinclusions.eu”) by one of the authors and is now permanently housed in the research collection of the Palaeo-Evo-Devo Research Group, Ludwig-Maximilians-Universtät, Munich, Germany (PED). One specimen came from the collection of the (Museum für Naturkunde Berlin, MfNB).

Further material was retrieved from the collection of the Center for Natural History in Hamburg (CeNak). A full list of the examined material is given in Table 1.

Information on syninclusions is provided in table 1 as well. All abbreviations of the collection names are according to the “The insect and spider collections of the world” website (Evenhuis, 2019).

For comparative purposes, we used extant larval representatives of Anisopodidae and Bibionidae (larvae, pupae, and adult) from the collection of the Zoological State Collection,

Munich (Zoologische Staatssammlung München, ZSM), in particular, *Sylvicola fenestralis* (Scopoli, 1763) (adult and pupa), *Mycetobia pallipes* Meigen, 1818 (larvae, pupae and adult, no collection number available) and *Penthetria funebris* Meigen, 1804 (larvae, pupae and adult, no collection number available) as well as *Bibio varipies* Meigen, 1830, (Centrum für Naturkunde Hamburg – CeNak, no collection number assigned).

The morphological terminology largely follows Borkent and Sinclair (2017). Yet, to enhance the understandability for non-experts, we amended some of the special morphological terms with more general terms. As Insecta is an accepted ingroup of Crustacea s.l. "crustacean"-terms are given in square brackets were necessary to provide wider frame correspondence.

Imaging methods

The specimens were imaged using a Keyence VHX-6000 Digital microscope, with ring-light type illumination and/or cross-polarised, co-axial illumination. All photographic images presented in this paper are composite images. Images were assembled using stitching and panorama functions to overcome the limitation of the field of view under higher magnifications. Each image details were recorded by a stack of images of shifting focus to overcome the limitation of the depth of field (Haug et al. 2008, 2011, 2013a). Fusion into sharp images and panorama stitching was performed with the built-in software (e.g. Haug et al. 2018, 2019). We also employed the built-in HDR function of the digital microscope; therefore every single frame is a composite from several images taken under different exposure times (cf. Haug et al. 2013b).

In addition to that, extant and fossil material was imaged using a Keyence BZ-9000 fluorescence microscope with either a 2x, 4x, 10x or 20x objective depending on the size of the objects. Observations were conducted at a wavelength of 532 nm since it was the most compatible with the fluorescence capacities of the fossil specimens (Haug et al. 2011). To counteract the limitation in the depth of the focus we recorded stacks of images which than were digitally fused to single in-focus images using CombineZP (GNU). Extant specimens were imaged using a ZEISS Stemi 508 Stereo Microscope (with 8:1 Zoom with double LED spot K and additional ring light) in combination with a DCM 510 ocular camera and. Photoshop Elements 11 was used to stitch different images to single panoramic images. The resulting images were post-processed in Photoshop Elements 11 software to optimize the histogram and sharpness as well as to amend the images with color markings to highlight morphological structures.

Two specimens (Dip-00653, Dip-00660) were scanned using X-Ray Computer tomograph Zeiss Xradia XCT-200 in the Zoological Institute and Museum of University of Greifswald. Scans were imaged in Drishti (Hörnig et al. 2016).

Micro-CT scanning on one specimen (MB.I.7295) was performed on a Nanotom m Phoenix (GE Sensing & Inspection Technologies GmbH). Scans were reconstructed to tiff stacks with the built-in software. Tiff stacks were further processed with ImageJ and Osirix 5.8.2 (Antoine Rosset; e.g. Haug et al. 2011; Nagler et al. 2017).

Morphometry

Maximum dorsal head capsule length and width of some larvae were measured, as suggested by Coomb et al. (1997) from photos, using ImageJ (public domain; Schneider et al., 2012). Statistical analysis of the data was performed in R (GNU), using the mblm-function of the mblm-package (Komsta, 2013).

Taxonomy

Wherever possible we decided not to use Linnean ranks ("rankless taxonomy"). Ranks represent arbitrary constructs in a way that they do not hold "comparative values" (Mayr, 1942, p. 291, line 3) and, in our view, do not contribute to an easier understanding of phylogenetic relations among species and higher groups. However, the rank of the genus is not as easy to dismiss as the ranks of higher (broader) systematic groups. This is solely due to its function as part of binomial species names. Even though there are ways to avoid this dilemma such as the application of uninomial nomenclature for species (Lanham, 1965) or the use of any higher systematic group (regardless ranked as genus or not) as part of the species name (Haug & Haug 2016 following Béthoux 2010), the traditional, rank based, application of binomial names is still required by the International Code of Zoological Nomenclature (ICZN, Chapter 2, Article 5 & App. B, 6.). To be consistent with the "Code" we establish a new generic name, even though there is only one species assigned to this name and thus the sole purpose of this name is to serve as part of the binomial species name. Hence, until a sister taxon (species or group) to the herein described species is found, the generic name is that of a monotypic taxon and thus no diagnosis can be given for it.

A single new species is described herein. It was registered in Zoobank. The electronic version of this article in Portable Document Format (PDF) will represent a published work according to the International Commission on Zoological Nomenclature (ICZN), and hence the new names contained in the electronic version are effectively published under that Code from the electronic edition alone. This published work and the nomenclatural acts it contains have been registered in ZooBank, the online registration system for the ICZN. The ZooBank LSIDs (Life Science Identifiers) can be resolved and the associated information viewed through any standard web browser by appending the LSID to the prefix http://zoobank.org/. The LSID for this publication is : urn:lsid:zoobank.org:pub:7E6FFA31-9DA8-44A6-BE7D-55E6AE34B660. The online version of this work is archived and available from the following digital repositories: PeerJ, PubMed Central and CLOCKSS.

Results

Taxonomy

Diptera Linnaeus, 1758

Bibonomorpha *sensu lato* Sensu Ševčík et al., 2016

Dinobibio gen.nov.

The LSID for this name is: urn:lsid:zoobank.org:act:8C8DCD9A-1A44-473E-9692-54C7AE204B91.

Etymology: from Ancient Greek δεινός (deinos), meaning 'terrible, potent or fearfully great', due to the imposing nature of the larva, which bears large protuberances, and the name of the extant ingroup of Bibionidae: *Bibio*.

Type species: *Dinobibio hoffeinseorum* sp. n. by present designation.

The LSID for this name is: urn:lsid:zoobank.org:act:80D4F834-D0D4-404F-AE02-C8FF184D4943

Remark: no diagnosis can be given, since the new generic name does not refer to a natural group but is only put up to provide a binomial name (see explanation above).

Dinobibio hoffeinseorum sp.n.
(Figs. 2A, 2B; 3A–D, Fig. S1)

Material examined: a single fossil larva from the GPIH collection (collection number GPIH-0024), which also is assigned as the holotype for the new species. The larva is well preserved, but lateral aspects obscured by the silvery film (probably air bubbles) covering parts of the trunk.

Syninclusions: a single "acalyptrate" fly ("Acalyptrata" = non-monophyletic assemblage of lineages within Brachycera that are not part of Calyptrata) is a syninclusion to the holotype.

Etymology: named after Christel and Hans-Werner Hoffeins for their immense contribution to the general study of dipterans preserved in Baltic amber Bibionidae in particular.

Description:

Habitus. Medium sized larva with a bowling-pin shaped body. Total length 6.4 mm. Body differentiated into presumably 20 segments, ocular segment plus 19 post-ocular segments.
Head. Ocular segment and post-ocular segment 1–5 (presumably) forming distinct capsule (head capsule). Head capsule longer than wide. Head capsule in dorsal view not accessible due to orientation of the specimen. Hind part of head capsule partly retracted into anterior trunk. Dimensions of head capsule: 860 µm long, width hard to access. Surface of head capsule with "warty" appearance, bearing numerous bulbous protrusions and smaller spine-like protrusions.
Ocular segment without apparent stemmata (larval eyes). Ocular segment recognizable by its appendage derivative – clypeo-labral complex. Clypeus (clypear sclerite) dome-shaped, with several bulbous expansions on the top, total length 260 µm, oval in general shape (Figs. 3A, 3B). Labrum not discernible.
Post-ocular segment 1 recognizable by its appendages, antennae [antennulae]. Antenna arising form head capsule postero-laterally to the clypeus. Antennae sitting on large piedestal (socket); no subdivision of antenna into elements apparent. (Figs. 3A-D)
Post-ocular segment 2 (intercalary segment) without externally recognizable structures. (Figs. 3A-D)
Post-ocular segment 3 recognizable by its pair of appendages, mandibles. Mandible only accessible at the distal tip, proximal part obscured. (Figs. 3A-D)
Post-ocular segment 4 recognizable by its appendage, maxilla [maxillula]. Maxilla massive, organised into proximal part and distal part, palp [endopod]. Proximal part differentiated into two lobes, outer lobe and inner lobe. Inner lobe, possible lacinia [endite]. Possible lacinia rectangular in outline. Possible lacinia 100 µm long, 200 µm wide. Palp arising from outer lobe, cylindrical, with two elements, palpomeres. Element 1 170 µm long. Element 1 Distally with

strong conical outgrowth. Outgrowth 80 µm long. Element 2 conical, 45 µm long, without apparent armature. (Figs. 3A-D)

Post-ocular segment 5 recognizable by its appendages, forming the labium [conjoined left and right maxillae]. Labium massive, heavily sclerotized, with proximal part and distal parts, palps [endopods]. Labium occupying over 60% of the total length of the head capsule ventrally. Palp cylindrical, total length 35 µm (Figs. 3C, 3D). Total length of the labium (without palp) 310 µm, width 200 µm.

Trunk. Trunk roughly bowling-pin shaped, diameter increasing posteriorly along the trunk, diameter of the trunk always larger than that of the head capsule (Figs. 2 A, B). Trunk with 12 visible units, interpreted as 3 thorax segments plus 8 abdominal units and a trunk end representing a conjoined structure of undifferentiated abdominal segments (9–11?). Trunk with abdominal units, progressively increasing in lateral aspect towards the posterior part of the body. Segment 1 1400 µm high, while 7th–1790 µm high. Trunk lacks parapodia and/or creeping welts. Trunk bears dozens of conical protuberances on the entire surface. Each segment of the trunk , with the exception of the trunk end, carries 8 prominent, fleshy protuberances dorso-laterally and ventrolaterally in groups of two, four at each side of the body. Protuberances widest at the mid-length, slightly narrower proximally part and tapering distally, mean length ca. 270 µm. Trunk surface with numerous small spines (Figs 2 A, B; Fig. S1). Trunk bears 10 pairs of spiracles (openings of the tracheal system) (Figs. 2, A,B;). Each spiracle situated in the centre of an elevated ridge (Figs. 2 A, B).

Thorax consists of three segments, pro-, meso- and methathorax.

Prothorax sub-equalin width to the head capsule, 670 µm. Prothorax bears a pair of large spiracles. Prothorax carries 8 prominent, fleshy protuberances dorso-laterally and ventrolaterally in groups of two, four at each side of the body.

Mesothorax 580 µm long. Mesothorax carries 8 prominent, fleshy protuberances dorso-laterally and ventrolaterally in groups of two, four at each side of the body; Mesothorax with no spiracle openings present.

Methathorax 560 µm long. Methathorax carries 8 prominent, fleshy protuberances dorso-laterally and ventrolaterally in groups of two, four at each side of the body. Methathorax bears a pair of spiracles (Figs 2 A, B; Fig. S1).

Abdomen (posterior trunk) Height of abdominal units progressively increasing in lateral aspect towards the posterior part of the body.

Abdominal unit 1 (abdomen segment 1) carries 8 prominent, fleshy protuberances dorso-laterally and ventrolaterally in groups of two, four at each side of the body; Abdominal unit 1 carries pair of spiracles laterally.

Abdominal unit 2 (abdomen segment 2) carries 8 prominent, fleshy protuberances dorso-laterally and ventrolaterally in groups of two, four at each side of the body; Abdominal unit 2 carries pair of spiracles laterally.

Abdominal unit 3 (abdomen segment 3) carries 8 prominent, fleshy protuberances dorso-laterally and ventrolaterally in groups of two, four at each side of the body; Abdominal unit 3 carries pair of spiracles laterally.
Abdominal unit 4 (abdomen segment 4) carries 8 prominent fleshy protuberances dorso-laterally and ventrolaterally in groups of two, four at each side of the body; Abdominal unit 4 carries pair of spiracles laterally.
Abdominal unit 5 (abdomen segment 5) carries 8 prominent fleshy protuberances dorso-laterally and ventrolaterally in groups of two, four at each side of the body; Abdominal unit 5 carries pair of spiracles laterally.
Abdominal unit 6 (abdomen segment 6) carries 8 prominent, fleshy protuberances dorso-laterally and ventrolaterally in groups of two, four at each side of the body; Abdominal unit 6 carries pair of spiracles laterally.
Abdominal unit 7 (abdomen segment 7) carries 8 prominent, fleshy protuberances dorso-laterally and ventrolaterally in groups of two, four at each side of the body; Abdominal unit 7 carries pair of spiracles laterally.
Abdominal unit 8 (abdomen segment 8) carries 8 prominent fleshy protuberances dorso-laterally and ventrolaterally in groups of two, four at each side of the body; Abdominal unit 8 lacks spiracles.
Trunk end (undifferentiated abdomen segments 9–11?) shorter than abdominal unit 8. Trunk end bears anus on the posterior part. Trunk end bears dozens of conical protuberances on the entire surface. No protuberances present in the immediate vicinity of the anus, on the postero-dorsal surface of the trunk end. Trunk end bears posterior spiracles with a single ecdysial scar (a site where the previous larval stage cuticle breaks from the spiracle)

Differential diagnosis: The larva is clearly different from any modern representative of Bibionidae based on the combination of the following characters: cylindrical body-shape; a maxillary palp with additional strong process distally on the element 1; trunk protuberances which are expanding towards mid length and then tapering again; terminal abdominal spiracle (abdominal segment 10), situated dorso-laterally; (Figs 2A, 2B; 3A–D).

Systematic interpretation, general body features: The general body shape, as well as absence of the ambulatory legs on the thorax, as well as the spiracle arrangement is consistent with this larvae being an immature stage of the group Diptera. The larval specimen GPIH-0024 is interpreted to be clearly closely related to Bibionidae based on the following combination of characters (see Fig. 4A–C; 5 A–C): Head capsule fully sclerotized, posterior part of it is retracted into the prothorax; maxilla very short and stocky, with short and strong maxillary palp, head capsule black and shiny; eyes absent, antenna rudimentary; tracheal system holopneustic ("type 1" spiracles on the prothorax and metathorax, as well as on abdominal segments 1–7 & 9). Body heavily sclerotized, yet head capsule is sclerotized even heavier than the body. Prothorax is the longest segment of the trunk (Skartveit, 2017).

The very long and robust labium, the body with fleshy protuberances, bearing two rows of the protuberances dorsally and a single ecdysial scar on the posterior spiracle specimen,

roughly resembles the condition in larvae of an ingroup of Bibionidae *Penthetria* Meigen, 1804 (Hennig, 1968, Skartveit, 2002) (Fig. 5A–C).

Systematic interpretation, head structures: The head capsule of the fossil larva is similar to that of larvae of Bibionidae. The antennae of the fossil larva are reduced as in larvae of Bibionidae. They are only represented by an undifferentiated conical piedestal in the fossil, similar to the condition in larvae of *Bibio* or *Penthetria* (both ingroups of Bibionidae; Fig. 5B, 5C). The maxilla of the fossil is robust, as it is in most larvae of Bibionidae. Yet the larva differs in the structure of the maxillary palp (Fig. 4B, 4C): it is robust and cylindrical in general shape, similar to the representatives of *Penthetria* or *Bibio* (Figs. 4A–C, 5A–C), but differs drastically from the representatives of both groups by bearing a conical outgrowth distally on the first element of the palp (Figs 3A–D, 4A–C, 5A–C). This outgrowth is somewhat similar to the structure on the palpi of some extant larvae Bibionidae. In particular, larvae of the ingroup of Bibionidae *Dilophus* possesses large, conical sensillae on the palpi. The outgrowth of the fossil larva is however much larger proportionally to the maxilla than that of larvae of *Dilophus.* Also it is situated on the distal part of the first element, not on the second element of the palp as it is the case for *Dilophus* (Krivosheina & Mamaev, 1967).

Other larval forms of Bibionomorpha, possessing large sensilla on the maxilary palps are larvae of fungus-gnats Mycomyinae (Mycetophilidae; Krivosheina & Mamaev, 1967: figs. 31:1, 31:6). In contrast to larvae of Mycomyinae however, the outgrowths of the fossil larva are not articulated. We therefore argue that this is an unique character which is a putative autapomorphy of *Dinobibio hoffeinseorum*.

The labium, in particular its proximal part, the mentum, is of the typical shape for larvae of Bibonidae (Figs. 3C, 3D), yet much broader and more robust than in any known larva of Bibionidae (s. 5A–C). The labium is occupying up to 60% of the entire width of the ventral area of the head, while the labium tin larvae of Bibionidae is much narrower, occupying about 20% of the ventral area of the head (Figs. 3 C, D, 5 B, C) (Skartveit, 2002). Mandibles and labrum are unavailable for a detailed examination due to being obscured by the other structures of the head.

Systematic interpretation, trunk structures: The general shape the body of the fossil larva is cylindrical with no parapods or other organs of locomotion (Fig 2A, 2B). Fleshy protuberances are protruding from the cuticle of the abdomen of the fossil larva. Numerous larvae of Bibionidae are exhibiting this condition as well. In particular, cuticular protuberances are typical for larvae of *Plecia* or *Penthetri*a (both ingroups of Bibionidae) (Figs. 5A–C).

The protuberances of *D. hoffeinseorum* however differ from the protuberances of known larvae of Bibionidae, by their characteristic shape. The proximal attachment of the protuberances is relatively narrow expanding towards midlength, and narrowing towards conical distal end. (Figs. 2A, 2B). That character is differentiating *D. hoffeinseorum* from larvae of Bibionidae. In the latter the protuberances are simply tapering towards the tip (Fig. 2B). Additionally, the largest protuberances of *D. hoffeinseorum* are situated at the thorax and abdominal segments 1 and 2, in contrast to most larvae of Bibionidae, in which the length of the protuberances is increasing towards the posterior (Figs. 2A, 2B, Fig. S1).

The tracheal system of the fossil larva is of the holopneustic type (“type 1”,10 pairs of spiracles: one on the prothorax, one on the metathorax, one pair at abdominal units 1-7, and one pair at the trunk end; sensu Hennig, 1968). A holopneustic tracheal system is characteristic for larvae of Bibionidae.

The spiracle openings of the fossil larvae are sitting on small elevated discs, representing a character state similar to that of some ingroups of Bibionidae. In larvae of Plecinae with spiracle openings sit on conical outgrowths (Figs. 4A, 5B, 5C; cf. Skartveit, 2017). Most of the spiracles are obscured by a silvery film, which, as it appears, formed by air, forced out from the tracheal system of the larva upon the entrapment in amber. Despite the obstruction of the view, the last tracheal spiracle pair (on abdominal unit 9) clearly has a single ecdysial scar, similar to larvae of *Penthetria* (Figs. 2A, 2B vs. 5A). Larvae of Bibionidae, have their posterior spiracles, being positioned posterior-laterally on the trunk end (Skartveit, 2002, 2017; Skartveit and Willassen, 1996). In contrast to them posterior spiracles of the new larva are situated at the anterio-dorsal part of the trunk end. Also, the posterior spiracles of the new larva are very small compared to the last spiracle of known larvae of Bibionidae.

In summary the fossil larvae, here described as *D. hoffeinseorum* differs from any known larva of Bibionidae in three key characters: 1) a strong process at the distal end of element I of the maxilar palp, 2) a dorso-laterally position of spiracle 10. (on the trunk end); (Fig. S1); protuberances of unique shape.

Systematic interpretation, summary: In fact, the larva described as *Dinobibio hoffeinseorum* is so different from known larval forms of Bibionidae concerning the general body pattern and the arrangement of the spiracles in the tracheal system, that it cannot be easily interpreted as an ingroup of Bibionidae (Skartveit, 2008, 2017).

We can think of two possible explanations for the distinctiveness of the *D. hoffeinseorum* in comparison to larvae of Bibionidae 1) *D. hoffeinseorum* is not an ingroup of Bibionidae, but rather sister species to the group. 2) *D. hoffeinseorum* is representing a highly derived branch of Bibionidae, that is now extinct.

Neither of these explanations can be conclusively excluded, until more material on the *D. hoffeinseorum* will become available, but it is beyond a doubt that this new species is very distinct from the rest of the known larvae of Bibionomorpha. The larvae of *D. hoffeinseorum* is exhibiting a curious mixture of traits, in this combination not known from any other larva of Diptera (cf. Kirk Spriggs and Sinclair, 2017). It does however possess the characters known from larvae Bibionidae and Mycetophylidae, yet in an unusual combination (i.e. see the discussion of the maxilla palpi element one outgrowth).

In fact, such “impossible” character combinations, are quite common in the fossil records, representing an “experimental” phase of evolution, when a number of traits were independently convergently evolving in different lineages (e.g. Haug et al., 2019). The unique combination of characters in *D. hoffeinseorum* is indicative of the active diversification in Bibionomorpha in the Eocene, which challenges the common view of the representatives of Insecta in the Baltic amber fossils as being “mostly modern” (Zherikhin, 2003).

Pachyneuridae Schiner, 1864
Pachyneura Zetterstedt 1838
(Figs. 6A, 6B, 7A, 7B, 8A–D)

Material: A single fossil larva from the collection of Carsten Gröhn which is now part of the CeNak (Hamburg) with the collection number GPIH-L-7516. Specimen moderately well preserved, with posterior parts of the trunk obscured by cracks, lateral view not available.

Syninclusions: "Stellate hairs" (oak leaf trichomes) are present as syninclusions to the single studied specimen.

Description:

Habitus. Medium sized larva with an dorso-ventrally flattened, spindle-shaped body. Total length 2.8 mm. Body differentiated into presumably 20 segments, ocular segment plus 19 post-ocular segments (Figs 6A, B, 7A, B).

Head. Ocular segment and post-ocular segment 1–5 (presumably) forming distinct capsule (head capsule). Head capsule wider than long. Hind part of head capsule not retracted into anterior trunk. Dimensions of head capsule : 450 µm long, 770 µm wide. Surface of head capsule smooth and glossy ocular segment without apparent stemmata (larval eyes) (9 A-D).

Ocular segment recognizable by its appendage derivative, clypeo-labral complex. Clypeus (clypear sclerite) roughly rectangular, 200 µm long, 380 µm wide. Labrum small, weakly sclerotized (Fig. 8C).

Post-ocular segment 1 without externally recognizable structures. Antenna not discernible, probably reduced. (Fig. 8A).

Post-ocular segment 2 (intercalary segment) without externally recognizable structures (Fig. 8C).

Post-ocular segment 3 recognizable by its pair of appendages, mandibles. Mandible total length 220 µm, with 3 strong teeth on the apex, apical and subapical teeth subequal (all ca. 22 µm in length), molar tooth shorter (16 µm) (Fig. 8C).

Post-ocular segment 4 recognizable by its appendage, maxilla [maxillula]. Maxilla massive, organised into proximal part and distal part, palp [endopod]. Very proximal region with sclerite (hypostomal bridge). Further distal proximal part differentiated into two lobes, outer lobe and inner lobe. Inner lobe possible lacinia [endite]. Possible lacinia rectangular in outline, 100 µm long, 70 µm wide. Palp arising from outer lobe, cylindrical, with two elements, palpomeres. Element 1 104 µm long, 45 µm long, with 4 hair-like setae distally (Fig. 8C).

Post-ocular segment 5 recognizable by its appendages, forming the labium [conjoined left and right maxillae]. Labium largely obscured by large possible lacinia (Fig. 8C).

Trunk with 12 visible units , interpreted as 3 thorax segments plus 8 abdominal units and a trunk end representing a conjoined structure of possibly undifferentiated abdominal segments (9–11?) (Figs 6A, B; 7 A, B). Trunk widest at about half of the length with 910 µm, diameter decreasing posteriorly to 280 µm. Trunk with elevated ridges (possible creeping welts) at units 1-6 (three thorax units, and first three units of the abdomen). Trunk surface with numerous small spines. Trunk bears 10 pairs of spiracles (openings of the tracheal system). Spiracles surrounded by lightly-coloured fields on the otherwise heavily sclerotized trunk units. Spiracles appear to have single ecdysial scars.

Thorax consists of three segments, pro-, meso- and methathorax.

Prothorax 80 µm long. Prothorax bears a pair of large spiracles. Prothorax subdivided into two parts by annular constriction.
Mesothorax 95 µm long. No spiracle openings present. Mesothorax bears two lateral setae (ca 70 µm long) on each side of the segment.
Methathorax 90 µm long. Methathorax bears two groups of dorsal setae (20-40 µm long), and two lateral setae (ca 70 µm long) on each side of the segment. Methathorax bears a pair of spiracles.
Abdomen (posterior trunk) Abdominal units progressively increasing in dorsoventral aspect towards the posterior part of the body, until reaching midlength of the abdomen, then decreasing again, towards the trunk end
Abdominal unit 1 (abdomen segment 1) bears two groups of dorsal setae (20-40 µm long), and two lateral setae (ca 70 µm long) on each side of the segment. Abdominal unit 1 carries a pair of spiracles laterally.
Abdominal unit 2 (abdomen segment 2) bears two groups of dorsal setae (20-40 µm long), and two lateral setae (ca 70 µm long) on each side of the segment. Abdominal unit 2 carries a pair of spiracles laterally.
Abdominal unit 3 (abdomen segment 3) bears two groups of dorsal setae (20-40 µm long), and two lateral setae (ca 70 µm long) on each side of the segment. Abdominal unit 3 carries a pair of spiracles laterally.
Abdominal unit 4 (abdomen segment 4) bears two groups of dorsal setae (20-40 µm long), and two lateral setae (ca 70 µm long) on each side of the segment. Abdominal unit 4 carries a pair of spiracles laterally.
Abdominal unit 5 (abdomen segment 5) bears two lateral setae (ca 70 µm long) on each side of the segment. Abdominal unit 5 carries a pair of spiracles laterally.
Abdominal unit 6 (abdomen segment 6) bears two groups of dorsal setae (20-40 µm long), and two lateral setae (ca 70 µm long) on each side of the segment. Abdominal unit 6 carries a pair of spiracles laterally.
Abdominal unit 7 (abdomen segment 7) bears two lateral setae (ca 70 µm long) on each side of the segment. Abdominal unit 7 carries a pair of spiracles laterally.
Abdominal unit 8 (abdomen segment 8) carries a pair of spiracles laterally.
Trunk end (undifferentiated abdomen segments 9–11?) obscured by cracks.

Systematic interpretation: The general body shape, as well as absence of the ambulatory legs on the thorax, and the spiracle arrangement is consistent with this larvae being an immature stage of Diptera. Numerous characters indicate that this is a larval form of Bibionomorpha: The larva possesses a very wide head capsule. The body as a whole is somewhat flattened dorso-ventrally, bearing six pairs of small ridges on the ventral side of the first six segments of the trunk (Figs. 6A, 6B, 7A, 7B).

The specimen is unusual by the combination of a holopneustic tracheal system (“type 2”: spiracles on the prothorax, metathorax and abdominal segments 1–8, Fig 6B), presence of long setae on the abdomen, the head capsule being wider than long and the prothorax (Figs. 6A, 6B, 7A, 7B), the latter being subdivided by a transversal furrow into the two rings (Figs. 6B, 7B). All

spiracles are surrounded by a lighter coloured area, in contrast to the more sclerotized parts of the segments. There are no other known larvae of Bibionomorpha with this state of characters. It is possible however that the lighter areas are actually taphonomic artefacts, caused by the air extrusion from the tracheal system upon the entrapment in amber.
The tracheal system with ten pairs of spiracles on the pro- and metathorax as well as on abdominal units 1–8 (Fig. 6B), is a synapomorphy of bibionomorphan ingroups Pachyneuridae + Hesperinidae (Krivosheina, 2012). The fossil however distinct from larvae of Hesperinidae by bearing a large number of long setae (up to 70 µm long) on the abdominal units. Larvae of Hesperinidae possess only very short setae (Kivosheina, 2012). *Pachyneura* (only ingroup of Pachyneuridae sensu Paramonov and Salmela 2015) includes two species *Pachyneura fasciata* Zetterstedt, 1838 and *P. oculata* Krivosheina & Mamaev, 1972. Due to the suboptimal preservation of the larva, we decided not to formally describe a new species, as the resulting holotype would be not optimal for future comparative work.

In general, based on the combination of morphological characters, the larva appears to be that of a typical larva of *Pachyneura* (Pachyneuridae see Paramonov and Salmela 2015). This is the first fossil record of Pachyneuridae sensu Paramonov and Salmela (2015). The sister group of Pachyneuridae+Hesperinidae – Cramptonomyiidae, is present in the fossil record with representatives of its ingroups *Tega* Blagoderov, Krzeminska and Krzeminski, 1993 and *Pivus* Blagoderov, Krzeminska and Krzeminski, 1993 from Upper Jurassic respectively the Lower Cretaceous of Asia (Blagoderov et al., 1993).

Anisopodidae Knab, 1912
Mycetobia Meigen, 1818

Material: 53 specimens of larvae and pupa in total were examined, see Table 1 for a complete list of the material. We were not able to distinguish distinct morphotypes for the larvae of *Mycetobia*, while for the pupae three distinct morphotypes are apparent.

Larvae
(Figs. 9 A-D; 10 A-E; Figs. S2-S10)

Material: see table 1 and Figs . 9 A-D; 10 A-E, Figs. S2-S10.

Description:
Habitus. Medium sized larva with roughly vermiform body (9 A, B). Total length 1.8–10.2 mm (all life stages; see table 2 for the summary of the morphometrics of the studied specimens) (10 A, B).
Body differentiated into presumably 20 segments, ocular segment plus 19 post-ocular segments (9 A-D, 10A-E).
Head. Ocular segment and post-ocular segment 1–5 (presumably) forming distinct capsule (head capsule). Head capsule longer than wide. Head capsule well developed, fully sclerotized dorsally, partially sclerotized ventrally. Hind part of head capsule not retracted into anterior

trunk. Dimensions of head capsule: length 99–512 µm (n=25, all life stages), width 85–420 µm (n=26, all life stages). Surface of head capsule smooth and glossy.

Ocular segment without apparent stemmata (larval eyes). Ocular segment recognizable by its appendage derivative, clypeo-labrum complex (Figs 10 A, D).

Post-ocular segment 1 recognizable by its appendages, antennae [antennulae]. Antenna represented by a single, cone-shaped element bearing a mushroom-like sensillum distally (Figs. 10 A, B, D, E).

Post-ocular segment 2 (intercalary segment) without externally recognizable structures (Figs. 10 A, B).

Post-ocular segment 3 recognizable by its pair of appendages, mandibles. Mandible divided into large, unsclerotized proximal portion, and heavily sclerotized distal portion, bearing numerous teeth. (Figs. 10 A, B, D,E).

Post-ocular segment 4 recognizable by its appendage, maxilla [maxillula]. Maxilla massive, organised into proximal part and distal part, palp [endopod]. Maxilla fleshy, very weakly sclerotized, only general outline visible. Proximal part differentiated into two lobes, outer lobe and inner lobe. Palp small, stump-like (Figs. 10 A, B).

Post-ocular segment 5 recognizable by its appendages, forming the labium [conjoined left and right maxillae]. Labium, especially proximal part (mentum), narrow and weakly sclerotized, trapezium-shaped. No distal structures (palpi) apparent. Posterior tentorial pits (external anchor point of the internal skeleton of the head capsule) present (Figs. 10 A, B).

Trunk. Trunk composed of 11 visible units: pro-, meso- and methathorax, 7 abdominal units and the trunk end. Trunk worm-like, units sub-equal in diameter (Figs. 9 A, B). Trunk lacks parapodia and/or creeping welts. Trunk bears two pars of spiracles: one on prothorax (Fig. 9 C) and one on trunk end (Figs. 9 C, D).

Thorax consists of three segments, pro-, meso- and methathorax.

Prothorax bears small, cone-shaped, anterior spiracles situated on posterolatero-dorsal surface. Prothorax subdivided into two unequal parts by annular constriction.

Meso-and **methathorax** subequal to prothorax in length, but without annular constriction (Figs. 9 A, B).

Abdomen (posterior trunk) Abdominal units are cylindrical, roughly equal to each other in diameter.

Abdominal unit 1 (abdomen segment 1) subdivided into two unequal parts by annular constriction.

Abdominal unit 2 (abdomen segment 2) subdivided into two unequal parts by annular constriction.

Abdominal unit 3 (abdomen segment 3) subdivided into two unequal parts by annular constriction.

Abdominal unit 4 (abdomen segment 4) subdivided into two unequal parts by annular constriction.

Abdominal unit 5 (abdomen segment 5) subdivided into two unequal parts by annular constriction.
Abdominal unit 6 (abdomen segment 6) subdivided into two unequal parts by annular constriction.
Abdominal unit 7 (abdomen segment 7) subdivided into two unequal parts by annular constriction.
Trunk end (undifferentiated abdomen segments 8–11?) subdivided into three unequal parts by two annular constrictions, with perianal shield (modified area of the last unit surrounding the anal aperture) on the ventral side. Trunk end bears posterior spiracles situated on the mediopostero-dorsal surface of the unit. Spiracular field surrounded by 5 short lobes, bearing no apparent hairs (Figs. 9 A-D).

Systematic interpretation :
The general body shape, as well as absence of the ambulatory legs on the thorax, and spiracle arrangement is consistent with this larvae being an immature stage of the group Diptera. The larvae further more show a distinct combination of characters: slender, vermiform body; head is sclerotized; dorsal part more strongly sclerotized than ventral one; mandible consists of fleshy proximal part more heavily sclerotised distal part; prothorax and abdominal units 1–7 each subdivided into two unequal parts by an annular constriction; respiratory system amphipneustic; anterior spiracles on a small cone on prothorax; posterior spiracles on the spiracular field, on the posterior of the trunk; trunk end covered by a perianal shield; the trunk end further subdivided into three parts.

This character combination matches the condition in larvae of Anisopodidae (window gnats). Furthermore the fossil larvae show a spiracular disc surrounded by only very short lobes and weak setae (Fig. 9 A–D, 11 A-D). This character is an autapomorphy of *Mycetobia* (ingroup of Anisopodidae).

Pupae

Morphotype 1
(Fig. 12 A, B; Figs. S11-S26)

Material: see table 1 and Fig. 12 A, B; Figs. S11-S26

Description:
Habitus. Medium sized pupa, with generally coma-shaped body in lateral view (Figs. 12 A, B; Figs. S11-S26). Pupae coloured roughly in the same colour as the matrix of the amber. Total length 2.7-5.1 mm long (n=14). See table 3 for the summary of the morphometrics. Body differentiated into presumably 20 segments, ocular segment plus 19 post-ocular segments.
Anterior part of the body, ocular segment and post-ocular segment 1–8 (presumably) forming a single globose unit (Figs. 12 A, B; Figs. S11-S26).

Ocular segment recognizable by its appendage derivative, clypeo-labrum complex and pair of large compound eyes. Labrum oval, slightly invaginated, membranous. Clypeus continuous with labrum (Figs. 12 A, B, Figs. 21). Frons (frontal sclerite) with a pair of short setae, situated on the top of small conical warts. Setae of the frontal sclerite longer than warts (Figs. 12 A, B; Fig. 21).
Post-ocular segment 1 recognizable by its appendages, antennae [antennulae]. Antenna consisting of 16 elements. Antennae moderately long, following the dorso-posterior outlines of the compound eyes.
Post-ocular segment 2 (intercalary segment) without externally recognizable structures (Figs. 12 A, B; Fig. S 21).
Post-ocular segment 3 without externally recognizable structures (mandibles) (Figs. 12 A, B; Sig. 21).
Post-ocular segment 4 recognizable by its appendage, maxilla [maxillula]. Maxilla organised into proximal part (non-serrated "lacinia") and distal part, palp [endopod] (Figs. 12 A, B; Fig. S 21).
Post-ocular segment 5 recognizable by its appendages, forming the labium [conjoined left and right maxillae]. Proximal parts of labium membranous, bears labial palps (Figs. 12 A, B; Fig. S 21).
Thorax consists of three segments, pro-, meso- and methathorax. Each bears a pair of (ambulatory) appendages (fore-, mid-and hind legs). Wings on mesothorax; halterae on methathorax. Thorax segments forming a single semiglobose structure, closely enveloping the head (Figs. 12 A, B; Fig. S 21).
Ambulatory appendages (legs) U-shaped folded, running between the wings: mid- and hind legs terminating above the mid-length of the first posterior trunk (abdomen) unit. Ambulatory appendages curving between the wing tips, and then, diverging again after passing the tips of the wings (Figs. 12 A, B; Figs. S 21, 25, 26). All ambulatory appendages comprised of following elements: coxa, trochanter, femur, tibia and tarsus subdivided into 5 elements.
Prothorax bears thoracic horns (modified spiracle 1). Thoracic horns club shaped, situated posterior to the eyes on the dorsal surface of the prothorax (Figs. 12 A, B). Prothorax bears 1st thoracic appendage pair (forelegs). Forelegs with femur and tibia forming a U-shaped loop, with highest point of the loop reaching the level at which maxillae arise
Mesothorax bears a pair of wings. Base of the wing aligned with the tip of the antennae. Midlegs underlying the forelegs, reaching beyond the tip of the wing.
Methathorax with a pair of spiracles. Hind legs underlying the forelegs and midlegs, reaching beyond the tip of the wing (Figs. 12 A, B).
Length of Head and thorax combined 1.0–2.3mm (n=14). Abdomen 1.8–3.6 mm long (n=14).
Abdomen (posterior trunk). With 9 units.
Abdominal unit 1 (abdomen segment 1) bearing two rings of strong hooklets.12 hooklets in the first ring, circa 70 hooklets in the second ring (Figs. 12 A, B).
Abdominal unit 2 (abdomen segment 2) bearing two rings of strong hooklets. 12 hooklets in the first ring, circa 70 hooklets in the second ring. Abdominal unit 2 bearing a pair of small spiracles (Figs. 12 A, B).
Abdominal unit 3 (abdomen segment 3) bearing two rings of strong hooklets.12 hooklets in the first ring, circa 70 hooklets in the second ring. Abdominal unit 3 bearing a pair of small spiracles (Figs. 12 A, B).

Abdominal unit 4 (abdomen segment 4) bearing two rings of strong hooklets.12 hooklets in the first ring, circa 70 hooklets in the second ring. Abdominal unit 4 bearing a pair of small spiracles (Figs. 12 A, B).
Abdominal unit 5 (abdomen segment 5) bearing two rings of strong hooklets.12 hooklets in the first ring, circa 70 hooklets in the second ring. Abdominal unit 5 bearing a pair of small spiracles (Figs. 12 A, B).
Abdominal unit 6 (abdomen segment 6) bearing two rings of strong hooklets.12 hooklets in the first ring, circa 70 hooklets in the second ring. Abdominal unit 6 bearing a pair of small spiracles (Figs. 12 A, B).
Abdominal unit 7 (abdomen segment 7) bearing two rings of strong hooklets.12 hooklets in the first ring, circa 70 hooklets in the second ring. Abdominal unit 7 bearing a pair of small spiracles (Figs. 12 A, B).
Abdominal unit 8 (abdomen segment 8) bearing two rings of strong hooklets.12 hooklets in the first ring, circa 70 hooklets in the second ring. Abdominal unit 7 bearing a pair of small spiracles (Figs. 12 A, B; Fig. S 21).
Trunk end (undifferentiated abdomen segments 9–11?) bears a pair of the lateral expansions (anal lobes) 8+2 hooklets. Hooklets arranged in 2 rings, two additional hooklets sitting on the anal lobes (Figs. 12 A, B; Fig. S 21). Abdomen length 1.7-3.6 mm (n=14).

Mycetobia pupa morphotype 2
(Figs.13 A, B, Fig. S 27)

Material: This morphotype was represented in our material by two pupae; one specimen in the amber piece GPIH-7514 from the collection of Carsten Gröhn, a second specimen was found in the amber piece PED-4866.

Description:
Habitus. Medium sized pupa, with generally coma-shaped body in lateral view. Pupa in whitish-green to brown colours. Total length 4.3–5.3 mm long (n=2).
Body differentiated into presumably 20 segments, ocular segment plus 19 post-ocular segments.
Head+thorax. Anterior part of the body composed of head and thorax, visible as a single globose structure (Figs 13 A, B; Fig. S 27).
Ocular segment and post-ocular segment 1–5 (presumably) forming distinct capsule (head capsule).
Ocular segment and post-ocular segment 1–5 (presumably) forming distinct caspule (head capsule). Ocular segment recognizable by its appendage derivative, clypeo-labrum complex and pair of large compound eyes. Labrum oval, slightly invaginated, membranous. Clypeus continuous with labrum (Figs 13 A, B; Fig. S 27). Frons (frontal sclerite) of post-ocular segment 1 with a pair of the short setae, situated on the top of small conical warts. Setae of the frontal sclerite shorter than warts.
Post-ocular segment 1 recognizable by its appendages, antennae [antennulae]. Antenna consisting of 16 elements. (Figs 13 A, B; Fig. S 27). Antennae moderately long, following the dorso-posterior outlines of the compound eyes.
Post-ocular segment 2 (intercalary segment) without externally recognizable structures.
Post-ocular segment 3 without externally recognizable structures (mandibles).

Post-ocular segment 4 recognizable by its appendage, maxilla [maxillula]. Maxilla organised into proximal part (non-serrated "lacinia") and distal part, palp [endopod].
Post-ocular segment 5 recognizable by its appendages, forming the labium [conjoined left and right maxillae]. Proximal part of labium membranous, bears labial palps (Figs 13 A, B; Fig. S 27).
Thorax consists of three segments, pro-, meso- and methathorax. Each bears a pairs of (ambulatory) appendages (fore, mid-and hind legs). Wings on mesothorax. Halterae on methathorax.
Thorax segments forming a single semiglobose structure, closely enveloping the head (Figs 13 A, B; Fig. S 27).
Ambulatory appendages (legs) U-shaped folded, running between the wings; mid- and hind legs terminating above the mid-length of the first posterior trunk (abdomen) unit. Ambulatory appendages do not curve between the wing tips, width of the legs stays constant, without divergence distally at the tips (Figs 13 A, B; Fig. S 27). All ambulatory appendages comprised of following elements: coxa, trochanter, femur, tibia and tarsus subdivided into 5 elements.
Prothorax bears thoracic horns (modified spiracle 1). Thoracic horns club shaped, situated posterior to the eyes on the dorsal surface. Forelegs superimposed over the thorax appendages 2 and 3, not reaching wings tip. Forelegs with femur and tibia forming a U-shaped loop, with highest point of the loop reaching the level at which maxillae arise.
Mesothorax bears a pair of wing. Antennae do not reach the base of the wing. Midlegs underlying the forelegs, reaching beyond the tip of the wing.
Methathorax bears a pair of halters and a pair of spiracles. Hindlegs underlying the forelegs and midlegs, reaching beyond the tip of the wing (Figs 13 A, B; Fig. S 27).
Length of head and thorax combined 1.9–2.2 mm (n=2).
Abdomen (posterior trunk). With 9 units.
Abdominal unit 1 (abdomen segment 1) bearing two rings of strong hooklets. Four hooklets in the first ring, circa 48 hooklets in the second ring.
Abdominal unit 2 (abdomen segment 2) bearing a pair of small spiracles. Abdominal unit 2 bearing two rings of strong hooklets. Four hooklets in the first ring, circa 48 hooklets in the second ring.
Abdominal unit 3 (abdomen segment 3) bearing a pair of small spiracles. Abdominal unit 3 bearing two rings of strong hooklets. Four hooklets in the first ring, circa 48 hooklets in the second ring.
Abdominal unit 4 (abdomen segment 4)bearing a pair of small spiracles. Abdominal unit 4 bearing two rings of strong hooklets .Four hooklets in the first ring, circa 48 hooklets in the second ring.
Abdominal unit 5 (abdomen segment 5)bearing a pair of small spiracles. Abdominal unit 5 bearing two rings of strong hooklets. Four hooklets in the first ring, circa 48 hooklets in the second ring.
Abdominal unit 6 (abdomen segment 6)bearing a pair of small spiracles. Abdominal unit 6 bearing two rings of strong hooklets.Four hooklets in the first ring, circa 48 hooklets in the second ring.
Abdominal unit 7 (abdomen segment 7)bearing a pair of small spiracles. Abdominal unit 7 bearing two rings of strong hooklets.Four hooklets in the first ring, circa 48 hooklets in the second ring.

Abdominal unit 8 (abdomen segment 8)bearing a pair of small spiracles. Abdominal unit 7 bearing two rings of strong hooklets.Four hooklets in the first ring, circa 48 hooklets in the second ring.
Trunk end (undifferentiated abdomen segments 9–11?) bears 6 hooklets, two at the anal lobes (Figs 13 A, B; Fig. S 27). Abdomen 2.7–3.2 mm long (n=2).

Mycetobia pupa morphotype 3
(Figs. 14 A, B; Figs. S 28, 29)
Material: Morphotype 3 is represented by 2 specimens, one actual pupa and one adult emerging from exuvium: table 1 and Figs. 14 A, B; Figs. S 28, 29.

Description:
Habitus. Medium-size insect pupae ,with generally coma-shaped body. Pupae brown. Total length 0.82–0.86 mm long (n=2). Body differentiated into presumably 20 segments, ocular segment plus 19 post-ocular segments (Figs. 14 A, B; Figs. S 28, 29).
Head+thorax. Anterior part of the body composed of head and thorax, visible as a single globose structure.
Ocular segment and post-ocular segment 1–5 (presumably) forming distinct capsule (head capsule). Ocular segment and post-ocular segment 1–5 (presumably) forming distinct capsule (head capsule). Ocular segment recognizable by its appendage derivative, clypeo-labrum complex and pair of large compound eyes. Labrum oval, slightly invaginated, membranous. Clypeus continuous with labrum (Figs. 22 A-C). Frons (frontal sclerite) with a pair of short setae, situated on the top of small conical warts (Figs. 14 A, B; Figs. S 28, 29).
Post-ocular segment 1 recognizable by its appendages, antennae [antennulae]. Antenna consisting of 16 elements. Antennae moderately long, following the dorso-posterior outlines of the compound eyes.
Post-ocular segment 2 (intercalary segment) without externally recognizable structures.
Post-ocular segment 3 without externally recognizable structures (mandibles) (Figs. 14 A, B; Figs. S 28, 29).
Post-ocular segment 4 recognizable by its appendage, maxilla [maxillula]. Maxilla organised into proximal part (non-serrated “lacinia”) and distal part, palp [endopod] (Figs. 14 A, B; Figs. S 28, 29).
Post-ocular segment 5 recognizable by its appendages, forming the labium [conjoined left and right maxillae]. Proximal part of labium membranose, bears labial palps (Figs. 14 A, B; Figs. S 28, 29).
Thorax consists of three segments, pro-, meso- and methathorax. Each bears a pairs of (ambulatory) appendages (fore, mid-and hindlegs). Wings on mesothorax. Halterae on methathorax.
Thorax segments forming a single semiglobose structure, closely enveloping the head of the pupa.

Ambulatory appendages U-shaped folded, running between the wings; mid- and hind legs terminating above the mid-length of the first posterior trunk (abdomen) unit. Ambulatory appendages curving between the wing tips, and then, diverging again after passing the tips of the wings (Figs. 14 A, B; Figs. S 28, 29). All ambulatory appendages comprised of following elements: coxa, trochanter, femur, tibia and tarsus subdivided into 5 elements.
Prothorax bears thoracic horns (modified spiracle 1). Thoracic horns club shaped, situated posterior to the eyes on the dorsal surface of the prothorax. Prothorax bears 1st thoracic appendage pair (forelegs). Forelegs superimposed over the thorax appendages 2 and 3, not reaching wings tip. Forelegs with femur and tibia forming a U-shaped loop, with highest point of the loop reaching the level at which maxillae arise (Figs. 14 A, B; Figs. S 28, 29).
Mesothorax bears a pair of wing. Midlegs underlaying the forelegs, reaching beyond the tip of the wing (Figs. 14 A, B; Figs. S 28, 29). Base of the wing aligned with the tip of the antennae. Hind legs underlying the forelegs and midlegs, reaching beyond the tip of the wing (Figs. 14 A, B; Figs. S 28, 29).
Methathorax bears a pair of halters and a pair of spiracles. Hindlegs underlying the forelegs and midlegs, reaching beyond the tip of the wing. Base of the wing aligned with the tip of the antennae.
Abdomen (posterior trunk) with 9 units.
Abdominal unit 1 (abdomen segment 1) bearing two rings of strong hooklets.12 hooklets in the first ring, circa 70 hooklets in the second ring.
Abdominal unit 2 (abdomen segment 2) bearing two rings of strong hooklets. 12 hooklets in the first ring, circa 70 hooklets in the second ring. Abdominal unit 2 bearing a pair of small spiracles.
Abdominal unit 3 (abdomen segment 3) bearing two rings of strong hooklets.12 hooklets in the first ring, circa 70 hooklets in the second ring. Abdominal unit 3 bearing a pair of small spiracles.
Abdominal unit 4 (abdomen segment 4) bearing two rings of strong hooklets.12 hooklets in the first ring, circa 70 hooklets in the second ring. Abdominal unit 4 bearing a pair of small spiracles.
Abdominal unit 5 (abdomen segment 5) bearing two rings of strong hooklets.12 hooklets in the first ring, circa 70 hooklets in the second ring. Abdominal unit 5 bearing a pair of small spiracles.
Abdominal unit 6 (abdomen segment 6) bearing two rings of strong hooklets.12 hooklets in the first ring, circa 70 hooklets in the second ring. Abdominal unit 6 bearing a pair of small spiracles.
Abdominal unit 7 (abdomen segment 7) bearing two rings of strong hooklets.12 hooklets in the first ring, circa 70 hooklets in the second ring. Abdominal unit 7 bearing a pair of small spiracles.
Abdominal unit 8 (abdomen segment 8) bearing a pair of small spiracles. Abdominal unit 7 bearing two rings of strong hooklets.Four hooklets in the first ring, circa 48 hooklets in the second ring.
Trunk end (undifferentiated abdomen segments 9–11?) bears a pair of the lateral expansions (anal lobes) and 8+2 hooklets. Hooklets arranged in 2 rings, two additional hooklets sitting on anal lobes (Figs. 14 A, B; Figs. S 28, 29). Abdomen length 0.5–0.6 mm (n=2).

Systematic interpretation (all 3 morphotypes):

Pupae of all three morphotypes possess a single pair of wings on the mesothorax and developing halterae on the methathorax identifying them as pupae of the group Diptera. They are interpreted as representatives of Anisopodidae based on the following combination of characters: slender; antennae long, reaching, at least until to the wing base; forelegs not reaching tip of wing, but mid and hindlegs reaching beyond the wings; thoracic horns small and oval to mushroom-like; spiracles present on metathorax and abdominal units 2–7. Last unit of abdomen bearing four pairs of strong denticles (Fig. 15 A–D).

Pupae of all three morphotypes possess characters autapomorphic for the group *Mycetobia* (ingroup of Anisopodidae): head bearing short frontal setae on conical warts; anterior and posterior margins of abdominal tergites bear rows of strong denticles.

Pupa morphotypes 1 and 2 can be distinguished from each other based on the number of denticles in the anterior row of the tergites, four in morphotype 2 and twelve in morphotype 1. Morphotype 1 can potentially include numerous species, indistinguishable in this stage and especially degree of preservation. Another diagnostic character differentiating the two morphotypes is the presence of a distal outward curvature of the legs of the morphotype 1, while morphotype 2 legs are of the constant width. Morphotype 3 is highly reminiscent of morphotype 1 but is significantly smaller, only about 30%.

Taxonomic attribution: The morphology of both the larvae and the pupae is entirely in line with corresponding stages of extant representatives of *Mycetobia.* At least some of the representatives of pupa morphotype 1 are representatives of *Mycetobia connexa*, which is the most abundant species of *Mycetobia* in the Baltic amber (Wojton et al., 2019). This is indicated by syninclusions in the amber piece PED-4395, which contains a single exuvium of a pupa of morphotype 1, as well as two adult representatives of Anisopodiae, a male and female (Figs. S 11, 15). This male is a representative of *Mycetobia*, based on the following combination of characters: wing without discal cell, vein Medial 3 branched, radial vein 2+3 ending in costa, radial vein 4+5 ending before the end of the costal vein, anal vein 1 very faint (Hancock, 2017). It is a representative of *Mycetobia connexa* Meunier, 1899 based on the following combination of characters: antenna elements (flagellomeres) 8–13 up to two time as long as wide; distal element of maxilary palp (palpomere) at most 3 times as long as wide, thinned; subcostal vein ending proximally to radial sector bifurcation; radial vein 1 ending on costal vein apex proximally of medial vein 1+2 bifurcation; fork of medial vein 1+2 wide; medial vein 1+2 elongated, as long as medial vein 1; medial vein 2 and medial vein 3+4 separated by a distance at least two times as the distance between ends of the medial vein 1 and medial vein 2; radial vein 2+3 two and 50% as long as radial sector or shorter; tarsus of foreleg 30% of the length of entire leg (including the coxa; Figs. S 11, 15) (Wojton et al., 2019a). We interpret the male and the female of the *Mycetobia* found in this piece as both being representatives of *M. connexa* based on the identical wing venation and similar antennae. We have associated the pupa exuvium with the adults, based on their proximity in amber (Figs. S 11, 15).

It is so far impossible to determine associations of the studied larvae with any of the seven species of *Mycetobi*a currently known from the Eocene European ambers (Wojton et al., 2019). Future records of pupa exuvia with emerging or pharate adults and/or associated larval exuvia may allow for the further life stages association. The record of three pupal morphotypes of *Mycetobia* in Baltic and Bitterfield amber is unsurprising, given relatively high species richness of *Mycetobia* in those Lagerstätten (Wojton, et al., 2019).

Anisopodidae Knab, 1912
Sylvicola Fatio, 1867
(Figs. 16 A–D)

Material: Single larva, in Baltic amber, DEI Dip-00641.

Description:
Habitus. Medium sized larva with roughly vermiform body. Total length 6.4 mm. Body differentiated into presumably 20 segments, ocular segment plus 19 post-ocular segments (Figs. 16 A–D).
Head. Ocular segment and post-ocular segment 1–5 (presumably) forming distinct caspule (head capsule). Head capsule longer than wide. Head capsule well developed, fully sclerotized dorsally, partially sclerotized ventrally. Head capsule in dorsal view not accessible due to orientation of the specimen. Hind part of head capsule not retracted into anterior trunk. Head capsule 280 µm long. Surface of head capsule smooth and glossy (Figs. 16 A–D).
Ocular segment without apparent stemmata (larval eyes). Ocular segment recognizable by its appendage derivative, clypeo-labrum complex. Labrum 70 µm long (Figs. 16 A–D).
Post-ocular segment 1 recognizable by its appendages, antennae [antennulae]. Antenna conical, consisting of one element, 44 µm long.
Post-ocular segment 2 (intercalary segment) without externally recognizable structures.
Post-ocular segment 3 recognizable by its pair of appendages, mandibles. Mandible only accessible at the distal tip, proximal part obscured. Mandible divided into large, unsclerotised proximal portion, and heavily sclerotized distal portion, bearing numerous teeth.
Post-ocular segment 4 recognizable by its appendage, maxilla [maxillula]. Maxilla massive, organised into proximal part and distal part, palp [endopod]. Proximal part of the maxilla fleshy, very weakly sclerotized, only general outline visible. Maxilla bears six cone-like outgrows, probably sensillae. Proximal part differentiated into two lobes, outer lobe and inner lobe (Figs. 16 A–D).
Post-ocular segment 5 recognizable by its appendages, forming the labium [conjoined left and right maxillae].
Trunk composed of 11 visible units: pro-, meso- and methathorax plus 8 abdominal units. Trunk worm-like, units sub-equal in diameter. Trunk lacks parapodia and/or creeping welts. Trunk bears two pars of spiracles, on prothorax and abdominal unit 8.
Thorax consists of three segments, pro-, meso- and methathorax.
Prothorax bears small, cone-shaped, anterior spiracles situated on posterolatero-dorsal surface. Prothorax subdivided into two unequal parts by annular constriction.
Meso-and **Methathorax** subequal to prothorax, but without spiracles.
Abdomen (posterior trunk). Abdominal units are cylindrical, roughly equal to each other in diameter (Figs. 16 A–D).

Abdominal unit 1 (abdomen segment 1) subdivided into two unequal parts by annular constriction.
Abdominal unit 2 (abdomen segment 2) subdivided into two unequal parts by annular constriction.
Abdominal unit 3 (abdomen segment 3) subdivided into two unequal parts by annular constriction.
Abdominal unit 4 (abdomen segment 4) subdivided into two unequal parts by annular constriction.
Abdominal unit 5 (abdomen segment 5) subdivided into two unequal parts by annular constriction.
Abdominal unit 6 (abdomen segment 6) subdivided into two unequal parts by annular constriction.
Abdominal unit 7 (abdomen segment 7) subdivided into two unequal parts by annular constriction.
Trunk end (undifferentiated abdomen segments 8–11?) subdivided into three unequal parts by two annular constrictions. Trunk end covered with perianal shield (modified area of the last unit surrounding the anal aperture) on the ventral side. Trunk end bears posterior spiracles situated on the mediopostero-dorsal surface of the unit. Spiracular field surrounded by five triangular, setose lobes.

Systematic interpretation: The general body shape, as well as absence of the ambulatory legs on the thorax, and the spiracle arrangement is consistent with this larva being an immature stage of the group Diptera. Numerous characters indicate that the specimen is a larva of the group Anisopodidae: body slender, vermiform; head fully sclerotized, dorsal part more strongly sclerotized than ventral; mandible with fleshy proximal heavily sclerotized distal part; prothorax and abdominal segments 1–7 subdivided into the two unequal parts by an annular constriction; respiratory system amphipneustic; anterior spiracle forming small cone on prothorax; posterior spiracles on spiracular field, on the posterior end; trunk end with perianal shield; the trunk end subdivided into three parts.

The fossil larva possesses a spiracular disc surrounded by triangular setose lobes. The character is autapomorphic for the group *Sylvicola* (ingroup of Anisopodidae). In larvae of other ingroups of Anisopodidae the spiracle is surrounded by roundish lobes, bare of setae. The structure of the spiracular disc can be used to distinguish between larvae of *Mycetobia* and *Sylvicola* (Hanckock, 2017) also in fossilized resin.

The Morphology of the fossil (Dip-00642) resembles extant larvae of *Sylvicola* to a high degree (cf. Keilin and Tate, 1940; Peterson,1981). Due to the preservation of the specimen no characters could be observed to reliably differentiate between the fossil larva from larvae of the extant species *Sylvicola fenestralis* (Scopoli, 1763). It is also impossible to differentiate to identify the larvae as a representative of any of the five known species of *Sylvicola* from Baltic amber, based on adults (Wojton, et al., 2018).

Syninclusions: stellate hairs and plant detritus are preserved in the same amber piece as the studied specimen.

Discussion

Species diversity and morphological diversity

Our investigations of Baltic and Bitterfeld amber material yielded at least four larval and three pupal morphotypes of Bibionomorpha. One larval type is even known from several instars.

There are probably numerous species of *Mycetobia* represented among the larval specimens. Yet, due to the degree of preservation it is impossible to distinguish them. The presence of several species within the material appears to be almost a certainty, taking into account the species diversity of Bibionomorpha in Baltic and Bitterfeld amber. represented by adult forms, including at least 12 species of Anisopodidae (Wojton et al., 2018, 2019a, 2019b). Also other bibionomorphan lineages show a quite rich fossil record in these amber Lagerstätten, again represented by adults, with at least 3 species of Hesperinidae, 10 species of Bibionidae and numerous species of the group Sciaroidea (Skartveit, 2002, 2008).

It is indeed surprising that the apparently abundant material of larvae and pupae of Bibionomorphan lineages in Eocene European amber has not attracted the attention of the scientific community earlier. There were some brief reports of pupae of Anisopodidae and Cecidomyiidae (Weitschat, 2009), but also these did not seem to attract much further attention. In a study by Haug et al. (2017), dealing with a group of dipteran pupae in a single amber piece, four specimens apparently representing morphotype 2 of *Mycetobia* have been reported (Haug et al., 2017), but misidentified as pupae of Asilidae, due to the somewhat similar structure of the spines or denticles on the trunk. Other pupae of Anisopodidae, without specification of further reaching taxonomic details have been reported from Miocene Dominican amber (Grimaldi, 1991).

No further immature stages of bibionomorphans have been reported from amber so far (Skartveit, 2017). This is probably a reflection of the fact, that in palaeoentomology, immature stages of the group Insecta seem often to be considered as 'inferior material' in comparison to adults. A possible reason for that is the relative difficulty of erecting new taxonomic entities based on larvae and pupae, which might act as disincentive in a field, where α-taxonomy is still seen as a pinnacle of research achievement (Azar et al., 2018).

Still, taking in account general scarcity of larval forms of Diptera preserved in amber (Andersen et al., 2015, Baranov et al., 2019), the high abundance of larvae of Bibionomorpha in Eocene European ambers is at least partly remarkable. The taphonomic window of the fossilized resins seems strongly biased towards flying, hence adult representatives of Insecta (or better Pterygota), especially for adult forms of Diptera (Solórzano Kraemer et al., 2015). Larvae of Diptera often live in aquatic habitats, soil, leaf litter or are internal parasites of plants and animals and thus have a limited opportunities for entrapment in plant resins and the subsequent preservation as amber inclusions (Solórzano Kraemeret al., 2015, Kirk-Spriggs, 2017).

Perkovsky et al. (2012) have shown that there is a stable structural cohort of animals preserved in Baltic and Rovno amber, which they termed “Sciara zone Diptera”, which made up to 20% of all inclusion in the representative batches of the Baltic and Rovno amber. “Sciara-zone Diptera” is represented mostly by flies of the groups Bibionomorpha and Tipulomorpha, possessing xylophagous or saprophagous larvae, which apparently were associated with the tree-trunks in the Baltic amber forest (Perkovsky et al., 2012). Larval forms of “Sciara-zone Diptera” and especially those of Anisopodidae are also living on tree trunks or right beneath them in the

upper leaf-litter. This makes their preservation in fact highly likely in comparison to other larval forms of Diptera (Hancock, 2017).

Such a high abundance of larvae and pupae of Bibionomorpha provides us an unprecedented look into the role of immature stages in the European Eocene amber forest. Since most of the immature stages of the Bibionomorpha in the studied material are closely reminiscent of corresponding stages of extant species, we can extrapolate the ecology of the fossil larval forms of Bibionomorpha to have been similar to their extant relatives (Seredszus and Wichard, 2008).

In fact, we have not been able to discern any substantial difference between studied larvae of the *Mycetobia*, *Sylvicola* and *Pachyneura* preserved in amber and their extant counterprarts. This is partially caused by the relatively low "resolution" of the characters on the fossil material, which does not allow us to recognize more subtle differences between fossil larvae and their extant relatives.

Extant larvae of Pachyneuridae are associated with dead wood in the pristine forests (Paramonov and Salmela, 2015). We assume a similar life habit for the fossil.

Extant larval representatives of *Mycetobia* and *Sylvicola* are associated with decaying organic material, mostly plant tissues, but dung or animal corpses might also be occasionally exploited (Hancock, 2017). We can therefore surmise that abundant larvae of *Mycetobia* (but also the larva of *Sylvicola*) preserved in Eocene amber were originally likewise connected to decaying organic matter. It is quite conceivable that a subtropical, seasonal forest in the Eocene of Europe would have an abundance of the decaying organic matter, in the form of leaf litter, dead plant or animal matter, bacterial biofilms and fungi (Hancock, 2017, Wojton et al., 2019b)

Ontogeny of the fossil forms of *Mycetobia*

The relatively large amount immature ("preimaginal") specimens of the species group ("genus") *Mycetobia*, enables us to do a limited quantitative analysis of the post-embryonic ontogeny of these flies (Fig. 17). Coombs et al. (1997) have shown that representatives of Anisopodidae have four larval stages in their development. This was not based on rearing larvae in the lab, but rather on looking at the distribution of several morphometric parameters. Head capsule length, head capsule width and body length have been measured for 303 larvae of *Sylvicola fenestralis* (Scopoli, 1763). Coombs et al. (1997) found that at least the head capsule width distribution followed a distinct four-peak pattern, corresponding to four supposed larval stages for this species.

'Dyar's rule', describes the pattern of larval development in Holometobola (Dyar, 1890). In particular, it describes the inter-moult growth within Holometabola occurring at a similar rate for each larval stage. As a short remark: this pattern even more general and not only true for Holometabola, but also for other crustaceans (cf. 'Brook's law', e.g. Fowler 1909). This strict pattern can be used to infer the number of larval stages from the available dataset on larval morphometry (Coombs et al., 1997). In particular, mean values for every size cohort of log-transformed datasets should follow a straight line, with high values of R^2. If the mean values behave differently, deviating from a straight line, this would result in a larval stage (size cohort) missing from the plot (Dyar, 1890; Coombs et al., 1997). Coombs et al. (1997) have shown that the factor, with that the head capsule width increases in-between the larval stages of *Sylvicola fenestralis*, remains relatively constant (0.57–0.66) and follows Dyar's rule (Dyar,1890; Coombs et al., 1997).

We applied the approach of Coombs et al. (1997) to our material and found that, when plotted at a histogram and arranged as a scatterplot (values plotted in increasing order; Figs. 18 A, 18 B) the head width and the head length of the fossil larvae of *Mycetobia* fall into four discrete categories (Figs. 19 A, 19 B). The line charted through the ordered dot-plot has 3 clear breaks for both the head length and the width of the head, but not for the body length (Fig. 19 B). This indicates the presence of four larval stages (based on head capsule width). We think that the absence of such breaks in the body length plot, is connected to the taphonomic conditions of the larvae. It is possible that upon death and preservation in amber larvae would shrink, obscuring body length of the living state.

We proceeded to calculate the mean value of the head width and length for each of the cohorts observed in the plot. Then, those mean values were plotted against the supposed larval stage. Coombs et al. (1997) and Dyar (1890) have shown that if the values of morphometric parameters plotted against the supposed number of the larval stages form a linear trend, that means that the sample analyzed contains all larval stages of the studied species (Fig. 17).

In our case, we have separated the stages based on the width of the head capsule, as Coombs et al. (1997) have shown it to be the most reliable predictor of the life-stage distribution in the measured larvae (Figs. 17, 18B). In our data the average values for both the head width and the head length form a perfect linearly increasing trend when plotted. The R^2 value for the head-width trend was 0.98 and 0.99 for the head length (Fig. 19).

Our data therefore support the presence of four larval stages in the larval development of species of *Mycetobia.* from the Eocene. The factor of growth between the stages was relatively steady, namely 0.6, consistent with Dyar's rule (Coombs et al., 1997; Table 2).

This is the first time that a full ontogenetic post-embryonic series of a dipteran could be reconstructed based on amber material A more incomplete series of single larval stage, pupa and adult was presented by Baranov et al. (2019). The reconstructed ontogeny of *Mycetobia* from amber demonstrates that during the Eocene Anisopodidae had linages with representatives exhibiting derived morphologies and morphological changes indistinguishable from extant forms of Anisopodidae (Wojton et al., 2019b).

Larvae of Bibionomorpha and amber forest ecology

Within the scientific community, a new understanding of the European Eocene amber forest (Schmidt e t al., 2019, Seyfullah et al., 2018) as a warm-temperate seasonal forest is currently emerging. This reconstruction is based on contemporary studies of paleobotanical species complexes, fungi and microorganisms as well as isotope signatures, preserved in these ambers (Schmidt e t al., 2019, Seyfullah et al., 2018). This reconstruction has currently not yet triggered a re-interpretation of the communities of Insecta in these amber, however it definitely will cause such a reinterpretation in the future.

The major weakness of the current interpretation of the palaeoecology of Insecta in Eocene amber, is that it is based on a very coarse application of the uniformitarism principle to the ecology of now extinct groups (Grund, 2006; Seredszus and Wichard, 2011; Zelentsov et al., 2012; Baranov et al., 2015). This means there is a mechanistic phylogenetic inference, in which fossil representatives of species groups ("genera") are automatically understood to have the autecological traits of the seemingly closest modern relatives. Yet, this is mere oversimplification, it is wrong and dangerous (Grund, 2006). Many authors, have shown that in case of large and ecologically "diverse genera", or "relic genera" (groups which which were much more diverse in the past), such inferences might lead to the widely inaccurate conclusions

(e.g. Stebner et al., 2018, Baranov et al., 2019). This problem is of course also a result of the (unreflected) use of taxonomical ranks, as a low rank (such as the genus) appears to suggest a close relationship among the species. However, the assignment of ranks is a completely arbitrary decision (Mayr, 1942) and neither reflects the age of a group nor the relatedness among species belonging to this group and as much less in a way that this would be comparable on a larger systematic scale (Dubois, 2007, Ereshefsky, 2002).

It is worth nothing in this aspect, that the paleoecology of many fossil species with aquatic larvae such as non-biting midges (Diptera, Chironomidae) or caddisflies (Trichoptera) is interpreted based on the larval ecology of their extant relatives, but inferred by fossils of the adults (for examples see Wichard et al., 2009). It is done in this way, a these groups of Insecta are widely used in aquatic biomonitoring today, and their larval habitats are thought to be rather narrow and well known (Merrit and Cummins, 1996).

The weakness of this approach to palaeohabitat reconstruction, is that it represents a type of double-inference, in case it is based on adults. First one infers a close relationship between the fossil (adult) animal and its extant relative with a known larval ecology assuming that the larvae of fossil adult animal are similar to their extant counterparts. Then we are inferring that the ecology of the fossil larvae would be close to its extant counterpart (Wichard et al., 2009).

A more direct interpretation of the ecology of larvae, which are more tied to particular habitats (and, in many forms of Insecta, perform most of the ecological functions within the life cycle) is considered advantageous in comparison to the above mentioned double-inference. Such an advantage arises from the direct observation of the larval morphology, which in combination with the interpretation of the taphonomic situation and syninclusions can tell us a lot about the ecology of an animal (Andersen et al., 2015; Baranov et al., 2019).

Hence the observed details of immature forms of Bibionomorpha eliminate one level of assumptions and provide more direct indications of the palaeo habitat. The high abundance of immatures of Anisopodidae in Eocene European amber forests, may indicate moist conditions and a large amount of decaying organic matter on the forest floor, a habitat characteristic for extant representatives of Anisopodidae (Hancock, 2017). This is reaffirming similar conclusions made based on the abundant presence of non-biting midges (Diptera, Chironomidae) with terrestrial larvae in Baltic amber (Andersen et al.,2015; Baranov et al.,2019). Secondly, the presence of a larva of Pachyneuridae (xylobiont-xylophages, living in the deep layer pf xylem of the old, still living trees) is indicative for pristine temperate forests (Krivosheina, 2006; Paramonov and Salmela, 2016). Hence, the findings of larval forms of Diptera provide a new independent source of information that can be used for palaeohabitat reconstruction.

Conclusions

This first examination of immatures of Bibionomorpha from Baltic and Bitterfeld amber is based on over 60 specimens, representing three major ingroups of Bibionomorpha: Bibionidae (at least possible sister group), Pachyneuridae and Anisopodidae. Bibionidae (or its sister species) and Pachyneuridae are both represented by a single larval morphotype each; Anisopodidae is represented by at least two larval morphotypes and at least three pupal morphotypes.

The larva of Pachyneuridae is the first fossil record for this group. The presence of this larva, indicates pristine, temperate forest conditions, with abundant old trees. That lines up well with emerging view on a Baltic amber forest as a warm-temperate, seasonal ecosystem (Schmidt et al., 2019).

Window Gnats (Diptera, Anisopodidae), are the most abundant immature stages of bibionomorphans in Bitterfeld and Baltic amber. A large number of fossil immatures allowed us to reconstruct the full post-embryonic ontogenetic series of fossil representatives of *Mycetobia* (Anisopodidae). This reconstruction only the second one dipterans in amber (first in Baranov et al., 2019), but more complete. It demonstrates that in the Eocene representatives of *Mycetobia*, just as their extant counterparts, had four larval stages.

This study shows the large potential of future studies on fossil larvae of flies in amber. Contrary to the widespread opinion, these larvae are relatively abundant. Their abundance, and ecological information associated with them (plus the additional information from syninclusions and other clues about the taphonomy), might be crucial to further elucidate the new, emerging picture of the palaeoecosystems that is preserved by Baltic and Bitterfeld amber.

Acknowledgements

VB is grateful to M. Spies and D. Doczkal (ZSM Munich) for his invaluable help with collection of ZSM as well as help with the literature. VB is grateful to M. K. Hörnig (University of Greifswald) for conducting MicroCt scanning of the Anisopodidae pupa. VB and JTH are grateful to C. & H.-W. Hoffeins (Hamburg), C. Gröhn (Hamburg) and U. Kotthoff (CeNak, Hamburg) for providing acess to the material.We are grateful to the editor and three anonymous reviewers for their efforts in improving this manuscript. Thanks to all people providing free software.

References

Andersen T, Baranov V, Goral T, Langton P, Perkovsky E, Sykes D. 2015. First record of a Chironomidae pupa in amber. *Geobios* 48(4): 281–286.

Armitage PD, Pinder LC, Cranston, P. S. (Eds.). 2012. *The Chironomidae: biology and ecology of non-biting midges*. Springer Science & Business Media, London.

Baranov V, Andersen T, Perkovsky, EE. 2015. Orthoclads from Eocene Amber from Sakhalin (Diptera: Chironomidae, Orthocladiinae). *Insect Systematics & Evolution* 46(4): 359–378.

Baranov V, Giłka W, Zakrzewska M, Jarzembowski E. 2019a. New non-biting midges (Diptera: Chironomidae) from Lower Cretaceous Wealden amber of the Isle of Wight (UK). *Cretaceous Research* 95: 138–145.

Baranov V, Hoffeins C, Hoffeins, H-W, Haug JT. 2019b. More than dead males: reconstructing the ontogenetic series of terrestrial non-biting midges from the Eocene amber forest. *Bulletin of Geosciences* 94(2): 1-13.

Béthoux, O. 2010. Optimality of phylogenetic nomenclatural procedures. *Organisms Diversity & Evolution* 10: 173–191 DOI: 10.1007/s13127-010-0005-3.

Blagoderov VA, Krzeminska E, Krzeminski W. 1993. Fossil and recent Anisopodomorpha (Diptera, Oligoneura): family Cramptonomyiidae. *Acta zoologica cracoviensia*, 35(3): 573–579.

Blagoderov V, Grimaldi DA, Fraser NC. 2007. How time flies for flies: diverse Diptera from the Triassic of Virginia and early radiation of the order. *American Museum Novitates* 3572: 1–39.

Borkent A., Sinclair BJ. 2017. Key to Diptera families-larvae. In: Kirk-Spriggs AH, Sinclair B J. (Eds.). *Manual of Afrotropical Diptera. Volume 1: Introductory chapters and keys to Diptera families*. *Suricata 4*. South African National Biodiversity Institute, Pretoria; pp. 357–405.

Coombs RM, Cleworth MA, Davies DH. 1997. Determination of instar for the window gnat Sylvicola Fenestralis (Diptera: Anisopodidae). *Water Research* 31: 186–193.

Dubois, A. 2007. Phylogeny, taxonomy and nomenclature: the problem of taxonomic categories and of nomenclatural ranks. *Zootaxa*, 1519(1): 27–_8.

Dyar HG. 1890. The number of molts of lepidopterous larvae. *Psyche: A Journal of Entomology* 5(175–176): 420–422.

Engel, M. 2019. Natural Histories. Innumerable insects. The stories of the most diverse and myriad animals on Earth. Sterling, New York.

Ereshefsky, M. 2002. Linnaean ranks: Vestiges of a bygone era. *Philosophy of Science*, 69(S3): S305–S315.

Evenhuis, N.L. 2019. The insect and spider collections of the world website. Available at: http://hbs.bishopmuseum.org/codens/ [Last accessed: 07.05.2019].

Fastovsky DE, Huang Y, Hsu J, Martin-McNaughton J, Sheehan PM, Weishampel DB. 2004. Shape of Mesozoic dinosaur richness. *Geology* 32: 877–880. https://doi.org/10.1130/G20695.1.

Fowler, G. H. 1909. Biscayan plankton collected during a cruise of H.M.S. 'Research' 1900. Part xii. The Ostracoda. Transactions of the Linnean Society of London (2), Zoology, x, pp. 219-336, 12 pls.

Grimaldi DA. 1991. Mycetobiine woodgnats (Diptera, Anisopodidae) from the Oligo-Miocene amber of the Dominican Republic, and Old World affinities. *American Museum novitates* 3014: 1–24.

Grimaldi D,Engel MS. 2005. *Evolution of the Insects*. Cambridge University Press.

Grund M. 2006. Chironomidae (Diptera) in Dominican amber as indicators for ecosystem stability in the Caribbean. *Palaeogeography, Palaeoclimatology, Palaeoecology* 241(3–4): 410–416.

Harris AC. 1983. An Eocene larval insect fossil (Diptera: Bibionidae) from North Otago, New Zealand. *Journal of the Royal Society of New Zealand* 13(3): 93–105.

Haug, C., Mayer, G., Kutschera, V., Waloszek, D., Maas, A. & Haug, J. T. 2011. Imaging and documenting gammarideans. International Journal of Zoology, art. 380829, DOI 10.1155/2011/380829

Haug, C., Shannon, K. R., Nyborg, T. & Vega, F. J. 2013b. Isolated mantis shrimp dactyli from the Pliocene of North Carolina and their bearing on the history of Stomatopoda. Bolétin de la Sociedad Geológica Mexicana 65, 273–284.

Haug, C., Herrera-Flórez, A. F., Müller, P. & Haug, J. T. 2019. Cretaceous chimera–an unusual 100-million-year old neuropteran larva from the "experimental phase" of insect evolution. Palaeodiversity 12, 1–11.

Haug, J. T., Haug, C. and Ehrlich, M. 2008. First fossil stomatopod larva (Arthropoda: Crustacea) and a new way of documenting Solnhofen fossils (Upper Jurassic, Southern Germany). Palaeodiversity, 1: 103–109.

Haug, J. T., Haug, C., Kutschera, V., Mayer, G., Maas, A., Liebau, S., Castellani, C., Wolfram, U., Clarkson, E. N. K. and Waloszek, D. 2011. Autofluorescence imaging, an excellent tool for comparative morphology. Journal of Microscopy, 244: 259–272.

Haug, J. T., Müller, C. H. G. and Sombke, A. 2013a. A centipede nymph in Baltic amber and a new approach to document amber fossils. Organisms Diversity and Evolution, 13: 425–432.

Haug, J. T. & Haug, C. 2016. "Intermetamorphic" developmental stages in 150 million-year-old achelatan lobsters – The case of the species tenera Oppel, 1862. *Arthropod Structure & Development* 45: 108–121 DOI: 10.1016/j.asd.2015.10.001.

Haug JT. in press. Why the term "larva" is ambiguous, or what makes a larva?. *Acta Zoologica early view*: 1–22.

Haug, J. T., Müller, P. & Haug, C. 2018. The ride of the parasite: a 100-million-year old mantis lacewing larva captured while mounting its spider host. Zoological Letters 4, 31.

Hancock EG. 2017. Anisopodidae (Wood Gnats or Window Gnats). In: Kirk-Spriggs, AH, Sinclair BJ. (Eds.). *Manual of Afrotropical Diptera. Volume 2: Nematocerous Diptera and lower Brachycera. Suricata* 5. South African National Biodiversity Institute, Pretoria; pp. 633–640.

Hennig W.1968 *Die Larvenformen Der Diptera. Teil 1*. Akademie-Verlag. Berlin.

Hörnig, M. K., Sombke, A., Haug, C., Harzsch, S. & Haug, J. T. 2016. What nymphal morphology can tell us about parental investment – a group of cockroach hatchlings in Baltic Amber documented by a multi-method approach. Palaeontologia Electronica 19(1), art. 5A, 20 pp.

International Commission on Zoological Nomenclature. 2012. Available at http://www.nhm.ac.uk/hosted-sites/iczn/code/ (accessed 2 May 2019).

Kalugina NS. 1974a. Eutrophication as one possible cause for the changes in aquatic biocenoses towards the end of the Mesozoic, pp. 137–139. In: *Antropogennoe evtrofirovanie vod [Anthropogenically eutrophied waters]*, Akademia Nauk SSSR, Chernogolov.

Kalugina NS. 1974b. Change in the subfamily composition of chironomids (Diptera, Chironomidae) as an indicator of possible eutrophication of bodies of water during the late Mesozoic. *Journal of the Moscow Naturalist's Society* 79: 45–56.

Kalugina NS, Kovalev VG. 1985. Jurassic Diptera of Siberia. *Izdatelstvo Nauka*, Moscow, 197 pp.

Knab F. 1912. New species of Anisopodidae (Rhyphidae) from Tropical America. [Diptera: Nemocera.]. *Proceedings of the Biological Society of Washington* 25:111–114.

Komsta L. 2013. mblm: median-based linear models. R package version 0.12.

Krivosheina NP. 2006. Taxonomic composition of dendrobiontic Diptera and the main trends of their adaptive radiation. *Zoologicheskii Zhurnal* 85 (7): 842–852. [in Russian]

Krivosheina M. 2012. Key to the families and genera of the Palearctic Dipterous insects of the suborder Nematocera, based on larvae [in Russian], Moscow, KMK Scientific press, 244 pp.+.

Krivosheina NP, Mamaev BM. 1967. *A Key to Dipteran Larvae Inhabiting Wood* [In Russian].Nauka Scientific Press, 266 pp.

Krivosheina NP, Mamaev BM. 1972. New data on relict Diptera of the Pachyneuridae family. Nauchnye Doklady vysshey shkoly. *Biological sciences* 11: 13–18. [in Russian].

Lanham, U. 1965. Uninominal nomenclature. *Systematic Zoology* 14: 144–144.

Mayr, E. 1942. *Systematics and the origin of species*. New York: Columbia University Press.

Marshall SA. 2012. *Flies. The natural history and diversity of Diptera*. Firefly Press Ltd, 616 pp.

Meigen JW. 1804. *Klassifikazion und Beschreibung der europäischen zweiflügligen Insekten. (Diptera Linn.). Erster Band, erste Abtheilung, mit VIII Kupfertafeln.* - pp. I–XXVIII [= 1–28], 1–152, Tab. I–VIII [= 1–8]. Braunschweig. (Reichard).

Meigen JW. 1818. *Systematische Beschreibung der bekannten europäischen zweiflügeligen Insekten. Erster Theil mit elf Kupfertafeln.* - pp. I–XXXVI [= 1–36], 1–324, [1]. Aachen. (Forstmann).

Merritt RW, Cummins KW. (Eds.). 1996. *An introduction to the aquatic insects of North America*. Kendall Hunt.

Mckenna DD, Wild AL, Kanda K, Bellamy CL, Beutel RG, Caterino MS, Farnum CW, Hawks DC, Ivie MA, Jameson ML, Leschen LAB, Marvaldi AE, McHugh JV, Newton AF, Robertson JA, Thayer MK, Whiting MF, Lawrance JF, Slipinski A, Maddison DR, Farrel, BD. 2015. The beetle tree of life reveals that Coleoptera survived end-Permian mass extinction to diversify during the Cretaceous terrestrial revolution. *Systematic Entomology* 40(4): 835–880. https://doi.org/10.1111/syen.12132

Nagler, C., Hyžný, M. & Haug, J. T. 2017. 168 million years old “marine lice” and the evolution of parasitism within isopods. BMC Evolutionary Biology 17, 76.

Perkovsky EE, Rasnitsyn AP, Vlaskin AP, Rasnitsyn SP. 2012. Contribution to the study of the structure of amber forest communities based on analysis of syninclusions in the Rovno Amber (Late Eocene of Ukraine). *Paleontological Journal* 46(3): 293–301.

Schneider CA; Rasband WS, Eliceiri KW. 2012. "NIH Image to ImageJ: 25 years of image analysis". *Nature methods* 9(7): 671–675.

Schiner IR. 1864. *Fauna Austriaca. Diptera.* Vol. II. Wien :C. Gerolds Sohn,1862-64.

Schmidt AR., Sadowski E-M, Kunzmann L, Kaasalainen U, Seyfullah LJ, Rikkinen J. 2019. Reconstruction of amber forests using plants, lichens and fungi: a case study of the ‘Baltic amber forest’. *Abstracts of th 8th International Conference on Fossil insects, Arthropods and Amber*. Santo-Domingo, 2019, 12–13

Scholtz, G. (2005) Homology and ontogeny: Pattern and process in comparative developmental biology. Theory in Biosciences124:121-143.

Scopoli JA. 1763. Entomologia Carniolica exhibens insecta Carnioliæ indigena et distributa in ordines, genera, species, varietates. Methodo Linnæana. pp. 1–420, [1]. Vindobonae. (Trattner).

Seredszus F, Wichard W. 2011. Overview and descriptions of fossil non-biting midges in Baltic amber (Diptera: Chironomidae). *Studia dipterologica* 17: 121–129.

Ševčík J, Kaspřák D, Mantič M, Fitzgerald S, Ševčíková T, Tóthová A, Jaschhof M. 2016. Molecular phylogeny of the megadiverse insect infraorder Bibionomorpha sensu lato (Diptera). *PeerJ:* 4, e2563.

Seyfullah LJ, Beimforde C, Dal Corso J, Perrichot V, Rikkinen J, Schmidt AR. 2018. Production and preservation of resins – past and present. *Biological Reviews* 93(3): 1684–1714.

Skartveit J. 2002. The larvae of European Bibioninae (Diptera, Bibionidae). *Journal of Natural History* 36(4): 449–485.

Skartveit J. 2009. Fossil Hesperinidae and Bibionidae from Baltic amber (Diptera: Bibionoidea). *Studia dipterologica* 15: 3–42.

Skartveit J. 2017. Bibionidae (March flies or Lovebugs). In: Kirk-Spriggs AH, Sinclair, BJ. (Eds.). *Manual of Afrotropical Diptera. Volume 2: Nematocerous Diptera and lower Brachycera. Suricata* 5. South African National Biodiversity Institute, Pretoria,pp. 497–504.

Skartveit J., Willassen E. 1996. Phylogenetic relationships in Bibioninae (Diptera, Bibionidae). Skarteveit, J. Studies on the systematics and life histories of Bibioninae (Diptera, Bibionidae). D. Phil. Thesis. University of Bergen, Bergen, Norway.

Solórzano-Kraemer MM, . Kraemer AS., Stebner F, Bickel DJ, Rust J. 2015. Entrapment bias of arthropods in Miocene amber revealed by trapping experiments in a tropical forest in Chiapas, Mexico. *PloSOne* 10(3): e0118820.

Stebner F, Baranov V, Zakrzewska M, Singh H, Giłka W. 2017. The Chironomidae diversity based on records from early Eocene Cambay amber, India, with implications on habitats of fossil Diptera. *Palaeogeography, Palaeoclimatology, Palaeoecology* 475: 154–161.

Wichard W, Gröhn C, Seredszus F. 2009. *Aquatic insects in Baltic amber - Wasserinsekten im Baltischen Bernstein*. Verlag Kessel, Remagen-Oberwinter. [in English and German].

Zelentsov NI., Baranov VA, Perkovsky EE, Shobanov NA. 2012. First records on non-biting midges (Diptera: Chironomidae) from the Rovno amber. *Russian Entomological Journal* 21: 79–87.

Zetterstedt JW. 1838. Sectio tertia. Diptera. Dipterologis Scandinaviae amicis et popularibus carissimus. Insecta Lapponica. Lipsiae [=Leipzig], 392 pp.

Ponomarenko, AG. 2003. Ecological evolution of beetles (Insecta: Coleoptera). *Acta zoologica cracoviensia* 46.Suppl (2003): 319-328.

List of figures

Figure 1. Phylogenetic relationship among different lineages of Bibionomorpha sensu lato, modified from Sevcik et al., 2016.

Figure 2. Dipteran larva, holotype of *Dinobibio hoffeinseorum* sp.n. GPIH, accession number (GPIH-0024) in lateral view. (A) overview, composite image. (B) coloured version of A above. Abbreviations: a1–a8, abdominal segment 1–8; hc, head capsule; mp, maxillary process; ms, mesothorax; mt, metathorax, pt, prothorax; s1-s10, spiracle 1–10; te, trunk end.

Figure 3. Fossil dipteran larva, holotype of *Dinobibio hoffeinseorum* sp.n. GPIH, accession number (GPIH-0024). (A) head capsule, latero-dorsal view; (B) coloured version of A. (C) head capsule, ventrolateral view. (D) coloured version of C. Abbreviations: an, antennae; cl, clypeus; hc, head capsule; lb, labium; md, mandible; mp, maxillary palp; mx, maxilla.

Figure 4. Extant larvae of Bibionidae. (A–B) *Bibio varipies* Meigen, 1830, CeNak, no collection number assigned. (C) *Penthetria funebris* Meigen, 1804, ZSM, no collection number assigned. (A) habitus ventral. (B) head capsule, ventral. (C) head capusle of fourth instar larva, ventral.

Figure 5 Extant larvae of Bibionidae. (A–C) *Penthetria funebris* Meigen, 1804, ZSM, no collection number assigned. A) fourth instar larva, habitus dorsal, arrows indicate the position of spiracles. (B) first instar larva, habitus ventral. (C) first instar larva, spiracle 1 (red arrow in B).

Figure 6. Fossil dipteran larva, *Pachyneura*, collection of GPIH, accession number (L-7617). (A) habitus, dorsal. (B) schematic drawing of habitus, dorsal. a2–a8, abdominal segment 2–8; cl, clypeus; Abbreviations: hc, headcapsule; ms, mesothorax; mt, metathorax; pt, prothorax; s1–s10, spiracle 1–10.

Figure 7. Fossil dipteran larva, *Pachyneura*, collection of GPIH (L-7617). (A) habitus, ventral. (B) coloured version of A. Abbreviations: a1–a8, abdominal segments 1–8; c1–c6, creeping welts 1–6; hc, headcapsule; lb, labrum; md, mandibles; mp, maxillar palp; ms, mesothorax; mt, metathorax; mx, maxilla; pt, prothorax; te, trunk-end.

Figure 8. Fossil dipteran larva, *Pachyneura*, collection of GPIH, accession number (L-7617). (A) head capsule, dorsal view. (B) head capsule, ventral view. (C) coloured version of B. (D) head capsule ventral view, schematic drawing. Abbreviations: hb, hypostomal bridge; hc, head capsule; lb, labrum; md, mandibles; mp, maxilarry palps; mx, maxillae.

Figure 9. Fossil dipteran larva, *Mycetobia*, DEI, accession number Dip-00640. (A) habitus, dorsal view. (B) coloured version of A. (C) posterior spiracles, specimen 2 of B. (D) coloured version of C. Abbreviations: a2–a8, abdominal segments 2–8; as, anterior spiracle; hc, head capsule; ms, mesothorax; mt, metathorax; ps, posterior spiracle; pt, prothorax.

Figure 10. Fossil dipteran larva, *Mycetobia*, DEI accession number Dip-00640, specimen 1 of Fig. 8B.(A) head capsule, dorsal view. (B) anterior spiracle. (C) coloured version of A. (D) head capsule, ventral view. (E) coloured version of D. Abbreviations: an, antenna; as, anterior spiracle; hc, head capsule; lb, labrum; md, mandibles; mn, mentum; mp, maxilar palps; mx, maxillae; ps, posterior spiracle.

Figure 11. Extant dipteran larva, *Mycetobia pallipes* Meigen, 1818, ZSM, no collection number assigned. (A) habitus, lateral. (B) coloured version of A. (C) head capsule, lateral view. (D) coloured version of C. Abbreviations: a2–a8, abdominal segment 2–8; as, anterior spiracle; hc, head capsule; md, mandible; mn, mentum; ms, mesothorax; mt, methathorax; mx, maxillae; pt, prothorax; tp, posterior pit of tentorium.

Figure 12. Fossil pupa, *Mycetobia connexa* (Mycetobia "morphotype 1"), GPIH, collection number 1851-DN. (A) habitus, ventro-lateral view. (B) coloured version of A. Abbreviations: a3–a7, abdominal segments 3–7; an, antennae; fs, frontal setae; p1, front legs; p2, midlegs; p3, hind legs; te, trunk-end; wn, wings.

Figure 13. Fossil pupa, *Mycetobia* "morphotype 2", PED, collection number PED-4866. (A) habitus, lateral view. (B) coloured version of A. Abbreviations: a1–a8, abdominal segments 1–8; an, antennae; ey, eyes; ms, mesothorax; mt, metathorax; p1, front legs; p2, midlegs; p, prothorax; te, trunk-end; th, thoracic horns; wn, wings.

Figure 14. Fossil pupa, *Mycetobia* "morphotype 3", pharate adult, DEI, collection number CCHH-DEI-608-2. (A) habitus, dorsal view. (B) habitus, ventral view.

Figure 15. Extant pupa, *Mycetobia pallipes* Meigen, 1818, ZSM, no collection number assigned, (A) habitus, dorsal view. (B) coloured version of A. (C) habitus, ventral view. (D) coloured version of C. Abbreviations: an-antennae; a3–a7, abdominal segments 3–7: ey, eyes; fs, frontal setae; mt, mesothorax; p1, front legs; p2, midlegs; p3, hind legs; te, trunk-end; th, thoracic horn; wn, wing.

Figure 16. Fossil larva, *Sylvicola*, DEI, collection number Dip-00642. (A) habitus, lateral view. (B) coloured version of A. (C) head capsule, lateral view. (D) coloured version of C. Abbreviations: a1–a8, abdominal segments 1–8; an, antennae; as, anterior spiracle; hc, head capsule; lb, labrum; md, mandible, mn, mentum; mx, maxilla; ms, mesothorax; te, trunk end.

Figure 17. Reconstructed ontogenetic sequence for representatives of *Mycetobia* in the Eocene.

Figure 18. Summary of statistical analysis. (A) biplot of fossil larvae of *Mycetobia* (n=36), head capsule length vs. head capsule width, red circles indicate hypothetical divisions into different larval stages based on the gaps in the data point distribution. I–IV, number of hypothetical larval stages. (B) distribution of the size cohorts within a sample of the fossil larvae of *Mycetobia*; upper-row-left, histogram of the head capsule width distribution (n=26); upper-row-center, histogram of the head capsule length distribution (n=25); upper-row-right, histogram of the body length distribution (n=36); lower-row-left, ranged plot (values ordered in ascending order) of the head capsule width, hypothetical division into different larval stages based on gaps in data point

distribution indicated with I–IV as numbers of supposed larval stages; lower-row-centered, ranged plot (values ordered in ascending order) of head capsule length; lower-row-right, ranged plot (values ordered in ascending order) of body length.

Figure 19. Natural logarithm of the mean larval head capsule width and head capsule of fossil larvae of *Mycetobia*, plotted against associated instar number.

SUPPLEMENTARY FIGURES

Figure S1. Fossil larva, holotype of *Dinobibio hoffeinseorum* sp.n. GPIH, accession number (GPIH-0024). (A) ventro-lateral view. (B) dorso-lateral view; (C1–C2) spiracle 10. (D1–D2) spiracle 2. (E1–E2) spiracle 1.

Figure S2. Fossil larvae, *Mycetobia* with syninclusions, GPIH, collection number GPIH-0247. (A) overview of the amber piece. (B) caddisfly male, Polycentropodidae. (C) partial syninclusion of an adult beetle. 1–4, larvae of *Mycetobia*; 5, beetle; 6–10 larvae of *Mycetobia*; 11, caddisfly male, Polycentropodidae

Figure S3. Fossil larvae, *Mycetobia* with syninclusions, collection number Dip-00640. (A) Overview of the inclusions. (B–D) dipterans, non-biting midges (Chironomidae). (B) *Rheosmittia pertenuis*, male. (C) Orthocladiinae, female. (D) *Rheosmittia pertenuis*, male, second specimen. (E) partial inclusions of *Mycetobia* sp. larvae. 1–4 Mycetobia larvae; 5–6 *R. pertenuis*, males; 7 Orthocladiinae, female.

Figure S4. Fossil larvae, *Mycetobia*, DEI, collection number Dip-00639. (A) habitus. (B) trunk end, with posterior spiracles. (C) head capsule, ventral view.

Figure S5. Fossil larvae, *Mycetobia*. (A) PED-5695. (B) DEI, collection number Dip-00654. (C) GPIH (BI-2350). (D) PED-4965.

Figure S6. Fossil larva, *Mycetobia* with syninclusions, collection of GPIH, collection number 3706-W. (A) mite. (B) fly, Phroidae. (C, D) larval specimen of *Mycetobia*. (C) ventral view. (D) dorsal view.

Figure S7. Fossil larvae, *Mycetobia*. A) Two specimens, GPIH (L-7592). (B) two specimens, GPIH (L-7592). (C) four specimens (1–4), PED, collection number PED-4748. (D) larva with syninclusions, PED, collection number PED-4970. 1, scale insect, (Coccoidea), nymph; 2, leaf hopper (Cicadellidae), nymph; 3, larva, *Mycetobia*; 4, non-biting midge (Chironomidae), female.

Figure S8. Fossil larvae, *Mycetobia*, DEI, collection number Dip-00649. (A) large larva. (B) specimens 1–3. (C) large larva.

Figure S9. Fossil larvae, *Mycetobia* with syninclusions. A) Overview of the amber piece Dip-00656from the collection of DEI. (B–D) larvae, *Mycetobia. (B) specimen 1. (C) specimen 2. (D) specimen 3.* 1, 2, 5, larva, *Mycetobia*; 3, 8, 10, 14 gall midges (Cecidomyiidae); 4, mite (Acari); 6, fly (“Acalyptrata”); 7, beetle (Coleoptera); 9, 11–13, ants (Fromicidae).

Figure S10. Fossil larvae, *Mycetobia*, DEI, collection number Dip-00655. (A) specimen 1. (B) specimen 2.

Figure S11. Fossil pupa (exuvium), *Mycetobia* "morphotype 1" with syninclusions, collection number PED-4395. (A) pupal exuvim of *Mycetobia* "morphotype 1". (B) *Mycetobia connexa*, female. (C) partial beetle (Coleoptera).

Figure S12. Fossil pupa, *Mycetobia connexa* (*Mycetobia* "morphotype 1"), GPIH collection number AKBS-00071. (A) habitus, ventro-lateral view. (B) abdomen, dorsal view.

Figure S13. Fossil pupa, *Mycetobia* "morphotype 1" with syninclusions, DEI, collection number Dip-00651. (A) habitus, lateral view. (B) dipteran non-biting midge (Chrionomidae, Orthocladiinae). (C) fly (Sciaroidea).

Figure S14. Fossil pupa, *Mycetobia connexa* (*Mycetobia* "morphotype 1") with syninclusions, GPIH, collection number 1851-DN. (A) pupa (exuvium), *Mycetobia* "morphotype 1" and fungus gnat (Keroplatidae) male. (B) fly (Sciaridae) male. (C) fly (Bibionomorpha, probably Anisopodidae).

Figure S15. Fossil pupa (exuvium), *Mycetobia connexa* (*Mycetobia* "morphotype 1") with syninclusions, collection number PED-4395. (A) Overview. (B) *Mycetobia connexa* male. (C) *Mycetobia connexa* male, distal part of metathoracic tibia. 1, *Mycetobia connexa* male; 2, *Mycetobia connexa* female; 3, pupal exuvium of *M. connexa*.

Figure S16. Fossil pupae, *Mycetobia* "morphotype 1". (A) DEI, collection number Dip-00657, dorsal view. (B) DEI, collection number Dip-00659, lateral view.

Figure S17. Fossil pupa, *Mycetobia* "morphotype 1", DEI, collection number Dip-00657 (Bitterfeld amber). (A) habitus, dorsal view. (B) habitus, ventral view.

Figure S18. Fossil pupa, *Mycetobia* "morphotype 1", DEI, collection number Dip-00655. (A) habitus, dorsal view. (B) habitus, ventro-lateral view.

Figure S19. Fossil pupa, *Mycetobia* "morphotype 1" with syninclusion, DEI, collection number Dip-00655 (specimen 2). (A) habitus, lateral view. (B) habitus, ventro-lateral view. (C) fly (Diptera, Sciaridae).

Figure S20. Fossil pupa (exuvium), *Mycetobia* "morphotype 1" collection number PED-4998. (A) habitus, ventral view. (B) habitus, dorsal view.

Figure S21. Fossil pupa (exuvium), *Mycetobia* "morphotype 1" (Bitterfeld amber), collection number Dip-00661. (A) habitus, ventral view. (B) habitus, dorsal view, (C) habitus, lateral view.

Figure S22. Fossil pupa, *Mycetobia* "morphotype 1" (Bitterfeld amber), DEI, collection number Dip-00650 . (A) habitus, dorsal view. (B) habitus, ventral view.

Figure S23. Fossil pupa, *Mycetobia* "morphotype 1" and syninclusions, GPIH, N-7095. A) overview. (B) pupa (upper left) *Mycetobia* "morphotype 1", (upper left) and larva of Neuroptera; lower right). (C, D) adult long-legged fly (Dolichopodidae). (C) specimen 1 (D) specimen 2.

Figure S24. Fossil pupa (exuvium), *Mycetobia* "morphotype 1", DEI, collection number Dip-00653. (A) habitus, dorsal view. (B) habitus, ventral view. (C) habitus, lateral view.

Figure S25. Fossil pupa (exuvium), *Mycetobia* "morphotype 1", rendering of µ-CT scans, DEI, collection number Dip-00653. (A) habitus, dorsal view. (B) habitus, ventral view. (C) habitus, lateral view.

Figure S26. Fossil pupa (exuvium), *Mycetobia* "morphotype 1", rendering of µ-CT scans , MfNB, collection number MB.I.7295 (A) habitus, dorsal view. (B) habitus, lateral view. (C) habitus, ventral view. (D) habitus, lateral view. All images red-blue stereo anaglyphs, please use red-cyan glasses to view.

Figure S27. Fossil pupae, *Mycetobia* and syninclusions. (A)"morphotype 1" and syninclusions, GPIH, collection number AKBS-00071. 1, largely unidentifiable (Insecta); 2, 3, 5–9, 13, 15 ant worker (*Lasius schiefferdeckeri* Mayr, 1868); 4, Fossil pupa, *Mycetobia* "morphotype 1"; 10 ant worker (*Ctenobethylus goepperti* (Mayr, 1868)). (B) syninclusions to "morphotype 2", PED, collection number PED-4866; adult rove beetle (Coleoptera: Staphylinidae), two adult gall midges (Diptera; Cecidomyiidae). (C) pupa of *Mycetobia* "morphotype 2", GPIH, collection number L-7514, habitus, ventral view.

Figure S28. Fossil pupa (pharate adult), *Mycetobia* "morphotype 3", rendering of µ-CT scans, DEI, collection number Dip-00660. (A) habitus, lateral view, right body side, mirrored. (B) habitus, lateral view, left body side. (C) habitus, dorsal view. (D) habitus, ventral view.

Figure S29. Fossil pupa (pharate adult), *Mycetobia* "morphotype 3" DEI, collection number Dip-00652. (A) habitus, dorsal view. (B) habitus, ventral view.

Table 1(on next page)

tables

Table 1. List of material examined

Table 2. Morphometry of the fossil Mycetobia larvae from Baltic and Bitterfeld ambers. Number in the parentheses after accession number indicates number of the Mycetobia syninclusion (if more than one in the same piece of amber). “L”- length, “W”-width.

Table 3. Morphometry of the fossil Mycetobia pupae from Baltic and Bitterfeld ambers. Number in the parentheses after accession number indicates number of the Mycetobia syninclusion (if more than one in the same piece of amber).

1 Table 1. List of material examined

ID-Number	Taxa	Specimens	Syninclusions	Deposited	Origin
GPIH-Schlee-0024	Dinobibio hoffeinseorum	1	Acalyptrata	GPIH	Baltic
Dip-00642	larvae Sylvicola (?)	1	Plant material+ stellate hairs	DEI	Baltic
PED-4395	Mycetobia connexa	male, female, pupal exuvia	partial inclusion of an adult beetle	PED	Baltic
BI-2350	Mycetobia larvae	1	none	GPIH	Bitterfeld
GPIH-3706 W	Mycetobia larvae	1	Phoridae adult+stellate hairs	GPIH	Baltic
Dip-00639	Mycetobia larvae	1		DEI	Baltic
PED-4965	Mycetobia larvae	1		PED	Baltic
PED-4970	Mycetobia larvae	1		PED	Baltic
PED-5695	Mycetobia larvae	1	Cicadellidae nymph, larva of Coccidoidea, worker ant and non-biting midge female (Diptera: Chironomidae: Tanytarsini)	PED	Baltic
GPIH-L-7592	Mycetobia larvae	2	Fragment of the Diptera Brachycera female, mites, stellate hairs	GPIH	Baltic
Dip-00640	Mycetobia larvae	3	2 males, 1 female Rheosmittia pertenuis	DEI	Baltic
PED-4748	Mycetobia larvae	4		PED	Baltic
GPIH-Schlee-0247	Mycetobia larvae	9	"Lepidoptera" (Trichoptera), + fragment of a beetle	GPIH	Baltic
AKBS-00071	Mycetobia pupa mt 1	1	Lasius schiefferdeckeri+Ctenobethylus geopperti	GPIH	Baltic
GPIH-1851DN	Mycetobia pupa mt 1	1	2 keratoplatidae males, sciaridae male+ probabbly male of Anisopodidae	GPIH	Baltic
Dip-00641	Mycetobia pupa mt 1	1	Plant material, insect tarsi fragment	DEI	Baltic
GPIH-N-7095	Mycetobia pupa mt 1	1	Neurothidae larvae, ants 2, Dolichopodidae flies x2, Trichoptera adult, insects i.s. x2	GPIH	Baltic
PED-4998	Mycetobia pupa mt 1	1	spider webs	PED	Baltic
GPIH-L-7514	Mycetobia pupa mt 2	1	Plant material +stellate hair	GPIH	Baltic
PED-4866	Mycetobia pupa mt 2	1	dult rove beetle (Coleoptera: Staphylinidae) and two adult gall midges (Diptera; Cecidomyiidae)	PED	Baltic
GPIH - 7516	Pachyneuridae larvae	1	stellate hairs	GPIH	Baltic
Dip-00649	Mycetobia larvae	5	Orthocladiinae female	DEI	Baltic
Dip-00650	Mycetobia pupa	1		DEI	Bitterfeld
Dip-00651	Mycetobia pupa	1		DEI	Baltic
Dip-00652	Mycetobia pharrate adult	1		DEI	Baltic
Dip-00653	Mycetobia pupa	1		DEI	Baltic
Dip-00654	Nematocera larvae sp	3		DEI	Baltic
Dip-00655	Mycetobia pup 2, 2 larvae	4	Adult sciaroidea, adult limoniidae	DEI	Baltic
Dip-00656	Mycetobia larvae	3	Ants, Cecidomyiidae,check photo	DEI	Baltic
Dip-00657	Mycetobia pupa mt1	1		DEI	Baltic
Dip-00658	Mycetobia larvae	1		DEI	Baltic
Dip-00659	Mycetobia pupa mt1	1		DEI	Baltic
Dip-00660	Mycetobia pharrate adult	1		DEI	Baltic
Dip-00661	Mycetobia pupa mt1	1		DEI	Bitterfeld

Dip-00662	Mycetobia pupa mt2	2		ZSM	extant
Dip-00663	Mycetobia pupa mt3	3		ZSM	extant
Dip-00664	Mycetobia pupa mt4	4		CeNak	extant
MB.I.7295	Mycetobia pupa mt1	1		MfNB	Baltic
NA	Mycetobia pallipes Meigen, 1818	>50		ZSM	Ober-Bayern, Fürstenfelderbruck, Roßkastanie, Wundausfluß, Bayern, Germany, 29.5-4.7.1994, leg. W. Schlacht.
NA	Penthetria funebris Meigen, 1804.	>50		ZSM	Augsburg, Lechau nördl. St. Stephan, Barb-F.,Auwald-Ruderal, 440 m, 27.05.1981,Schmidt.
NA	*Bibio varipies* Meigen, 1830	1		CeNak	NA

2

3 Table 2. Morphometry of the fossil Mycetobia larvae from Baltic and Bitterfeld ambers. Number
4 in the parentheses after accession number indicates number of the Mycetobia syninclusion (if
5 more than one in the same piece of amber). “L”- length, “W”-width.

Acession number	L total, µm	head L, µm	head W, µm	larval stage
Dip-00640 (1)	2676.177	145.201	105.129	1
GPIH-0247/8	3346.186	165.624	115.993	1
PED-4748(3)	2283.494	99.005	87.693	1
Dip-00656	2067	166	115	1
Dip-00640 (2)	2151.442	186.238	162.515	2
Dip-00640(3)	2693.354	209.082	178.836	2
Dip-00640 (4)	2405.655	171.311	155.919	2
GPIH-3706 W	2957.863	190.825	180.487	2
BI2350	3909.86	235.719	155.103	2
GPIH-0247(7)	3034.273	195.118	166.481	2
PED-4748(1)	5048.093	309.328	171.883	2
PED-4970	4591.883	233.701	156.178	2
Dip-00656(2)	2784	181	192	2
Dip-00655(1)	2364	139	145	2
Dip-00649(1)	5166	178	181	2
GPIH-0247(9)	3	320.337	259.113	3
PED-4748(2)	5207.932	388.551	246.06	3
PED-4748(4)	10222.51		191.139	3
PED-4965	7027.351	319.331	218.775	3
PED-5695	5503.7	284.294	230.87	3
Dip-00639	7609.245	306.751	295.106	3
Dip-00658	8139	376	239	3
Dip-00656 (1)	5693	266	240	3
Dip-00655(2)	2344	225	227	3

Dip-00649(2)	8385	352	277	3
GPIH-0247(2)	3929.665	512.765	418.808	4
GPIH-0247(1)	5328.197	NA	NA	NA
GPIH-0247(3)	4150.859	NA	NA	NA
GPIH-0247(4)	4898.89	NA	NA	NA
GPIH-0247(5)	1819.851	NA	NA	NA
GPIH-0247(6)	3486.205	NA	NA	NA
GPIH-l-7592(1)	7194.75	NA	NA	NA
GPIH-l-7592(2)	6096.312	NA	NA	NA
GPIH-l-7592(3)	5701.261	NA	NA	NA
GPIH-l-7592(4)	6454.761	NA	NA	NA
GPIH-l-7592(5)	4017.086	NA	NA	NA

Table 3. Morphometry of the fossil Mycetobia pupae from Baltic and Bitterfeld ambers. Number in the parentheses after accession number indicates number of the Mycetobia syninclusion (if more than one in the same piece of amber).

Accession number	**length, µm**	**parameter**	**Morphotype**
Dip-00655	1777.074	abdomen	morphotype 1
Dip-00655	1013.289	thorax+head	morphotype 1
Dip-00655	2679.723	total	morphotype 1
Dip-00655	2484.743	abdomen	morphotype 1
Dip-00655	1614.781	thorax+head	morphotype 1
Dip-00655	3842.338	total	morphotype 1
Dip-00652	362.857	thorax+head	morphotype 3
Dip-00652	527.673	abdomen	morphotype 3
Dip-00652	826.356	total	morphotype 3
Dip-00653	2420.659	abdomen	morphotype 1
Dip-00653	1779.554	thorax+head	morphotype 1
Dip-00653	3919.83	total	morphotype 1
GPIH-1851DN	3021.056	abdomen	morphotype 1
GPIH-1851DN	2266.877	thorax+head	morphotype 1
GPIH-1851DN	5059.427	total	morphotype 1
Dip-00641	2340.723	abdomen	morphotype 1
Dip-00641	1624.223	thorax+head	morphotype 1
Dip-00641	3876.262	total	morphotype 1
Dip-00650	320.106	thorax+head	morphotype 3
Dip-00650	645.888	abdomen	morphotype 3

Dip-00650	864.21	total	morphotype 3
Dip-00660	2935.409	abdomen	morphotype 1
Dip-00660	1924.388	thorax+head	morphotype 1
Dip-00660	4238.969	total	morphotype 1
Dip-00661	3647.714	abdomen	morphotype 1
Dip-00661	2220.334	thorax+head	morphotype 1
Dip-00661	5861.01	total	morphotype 1
Dip-00657	2310.204	abdomen	morphotype 1
Dip-00657	1453.298	thorax+head	morphotype 1
Dip-00657	3835.301	total	morphotype 1
GPIH-N-7095.	2154.926	abdomen	morphotype 1
GPIH-N-7095.	1710.244	thorax+head	morphotype 1
GPIH-N-7095.	3761.555	total	morphotype 1
Dip-00659	2466.357	abdomen	morphotype 1
Dip-00659	1697.196	thorax+head	morphotype 1
Dip-00659	3744.385	total	morphotype 1
Dip-00651	2187.597	abdomen	morphotype 1
Dip-00651	1543.324	thorax+head	morphotype 1
Dip-00651	3343.985	total	morphotype 1
AKBS-00071	2490.055	abdomen	morphotype 1
AKBS-00071	1784.352	thorax+head	morphotype 1
AKBS-00071	3630.701	total	morphotype 1
PED-4395	2081.768	abdomen	morphotype 1
PED-4395	1561.697	thorax+head	morphotype 1
PED-4395	3528.726	total	morphotype 1
PED-4866	2596.66	thorax+head	morphotype 2
PED-4866	3041.19	abdomen	morphotype 2
PED-4866	5379.843	total	morphotype 2
PED-4998	2882.949	abdomen	morphotype 1
PED-4998	2174.641	thorax+head	morphotype 1
PED-4998	4811.619	total	morphotype 1
GPIH-L-7514	1826.663	thorax+head	morphotype 2
GPIH-L-7514	2936.171	abdomen	morphotype 2
GPIH-L-7514	4858.746	total	morphotype 2

Figure 1

Phylogenetic relationship among different lineages of Bibionomorpha sensu lato, modified from Sevcik et al., 2016.

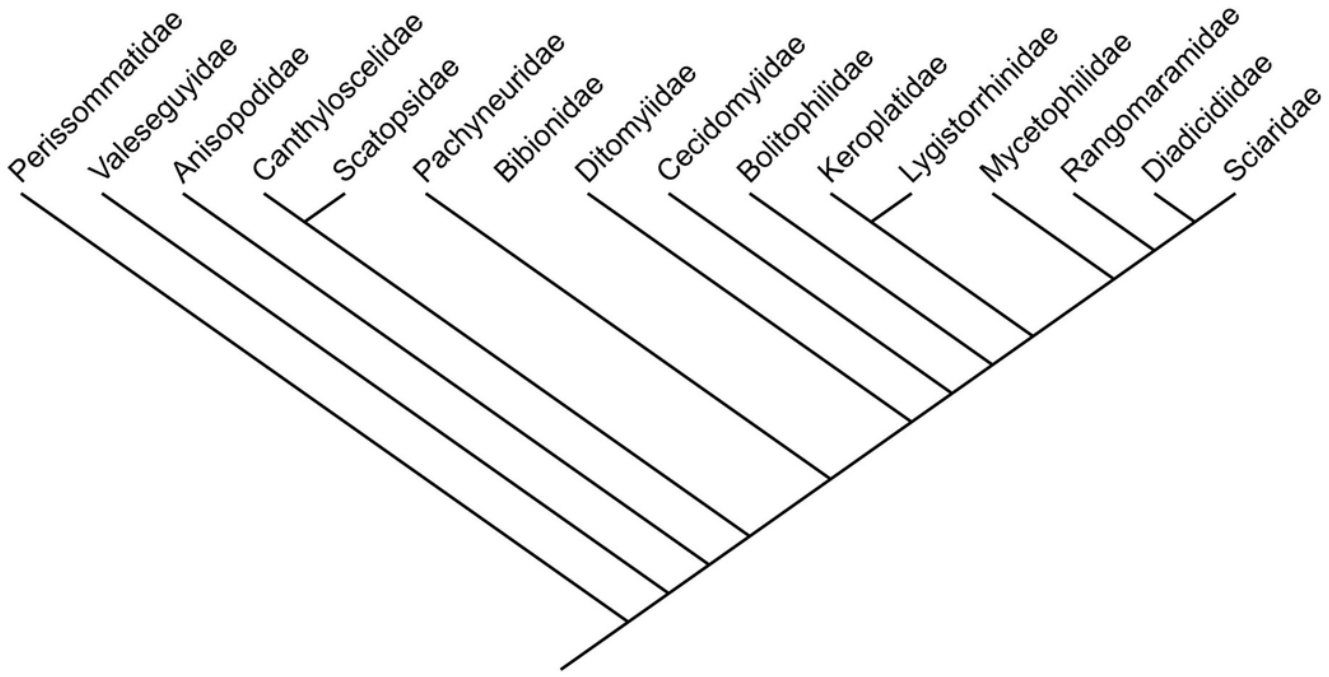

Figure 2

Dipteran larva, holotype of *Dinobibio hoffeinseorum* sp.n. GPIH, accession number (GPIH-0024) in lateral view.

(A) overview, composite image. (B) coloured version of A above. Abbreviations: a1–a8, abdominal segment 1–8; hc, head capsule; mp, maxillary process; ms, mesothorax; mt, metathorax, pt, prothorax; s1-s10, spiracle 1–10; te, trunk end.

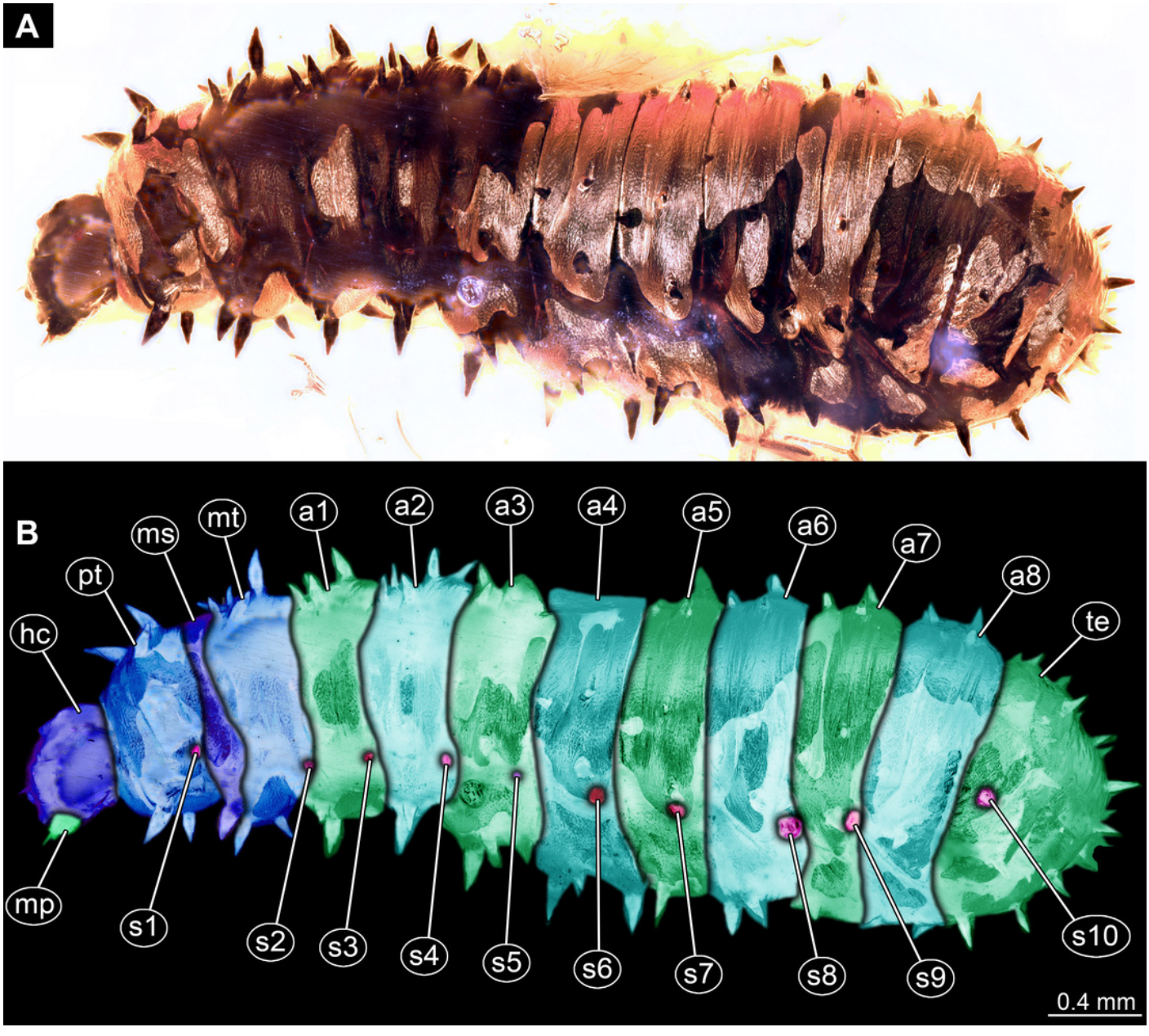

Figure 3

Fossil dipteran larva, holotype of *Dinobibio hoffeinseorum* sp.n. GPIH, accession number (GPIH-0024).

(A) head capsule, latero-dorsal view; (B) coloured version of A. (C) head capsule, ventrolateral view. (D) coloured version of C. Abbreviations: an, antennae; cl, clypeus; hc, head capsule; lb, labium; md, mandible; mp, maxillary palp; mx, maxilla.

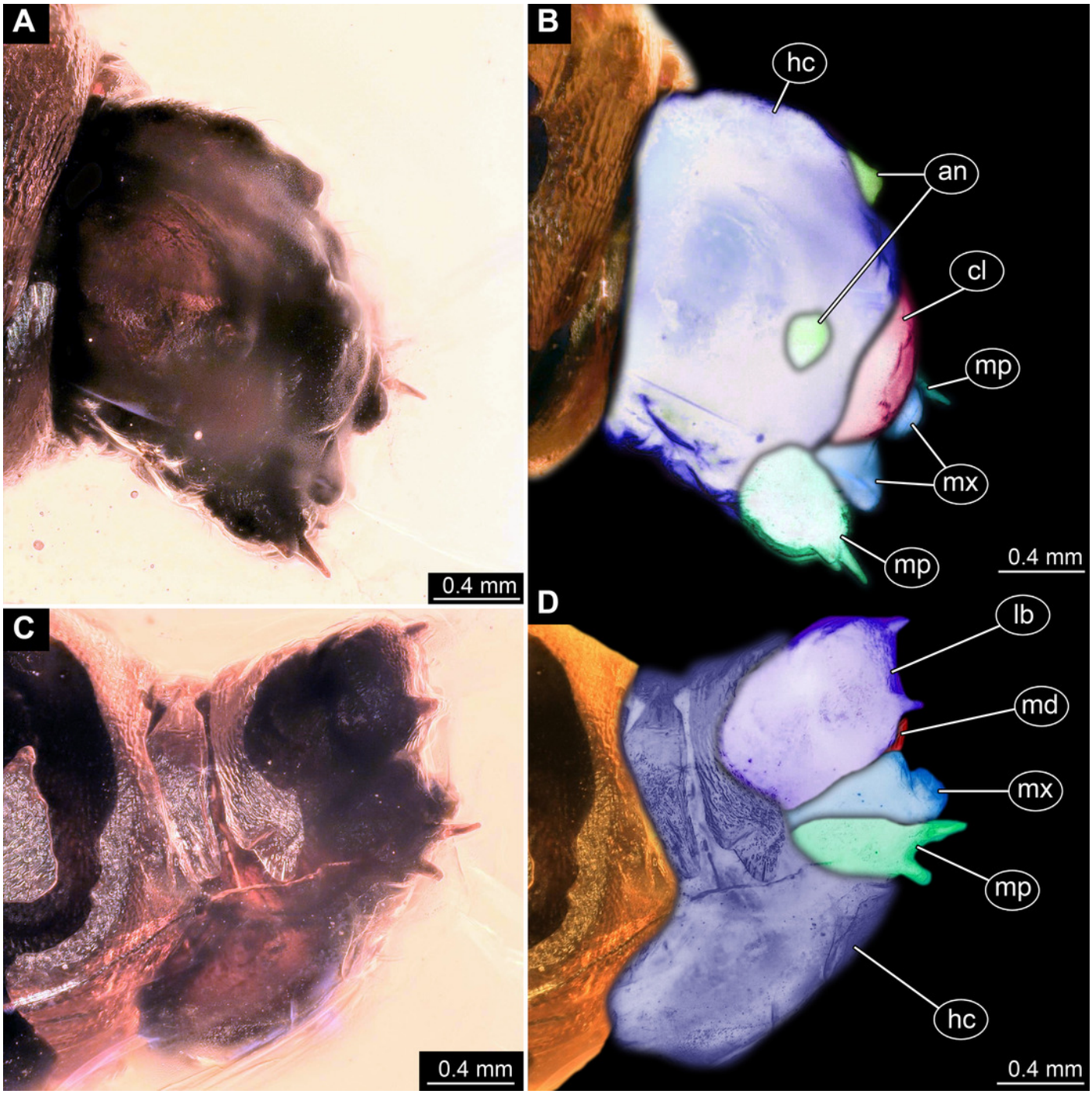
A
0.4 mm
B
hc
an
cl
mp
mx
mp
0.4 mm
C
0.4 mm
D
lb
md
mx
mp
hc
0.4 mm

Figure 4

Extant larvae of Bibionidae. (A–C) *Bibio varipies* Meigen, 1830, CeNak, no collection number assigned.

(A) *Penthetria funebris* Meigen, 1804, ZSM, no collection number assigned. (A) habitus ventral. (B) head capsule, ventral. (C) head capusle of fourth instar larva, ventral.

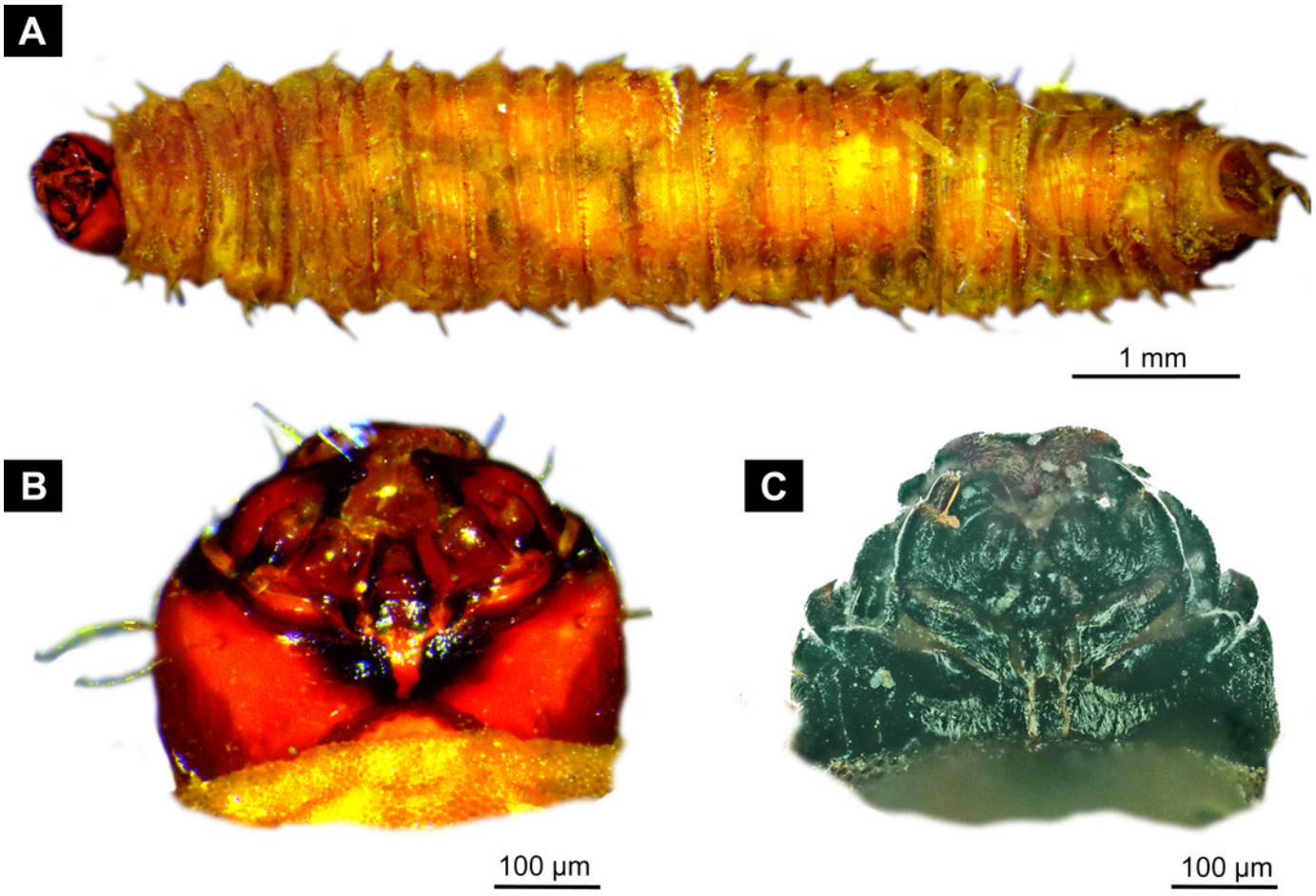

Figure 5

Extant larvae of Bibionidae. (A–C) *Penthetria funebris* Meigen, 1804, ZSM, no collection number assigned.

A) fourth instar larva, habitus dorsal, arrows indicate the position of spiracles. (B) first instar larva, habitus ventral. (C) first instar larva, spiracle 1 (red arrow in B).

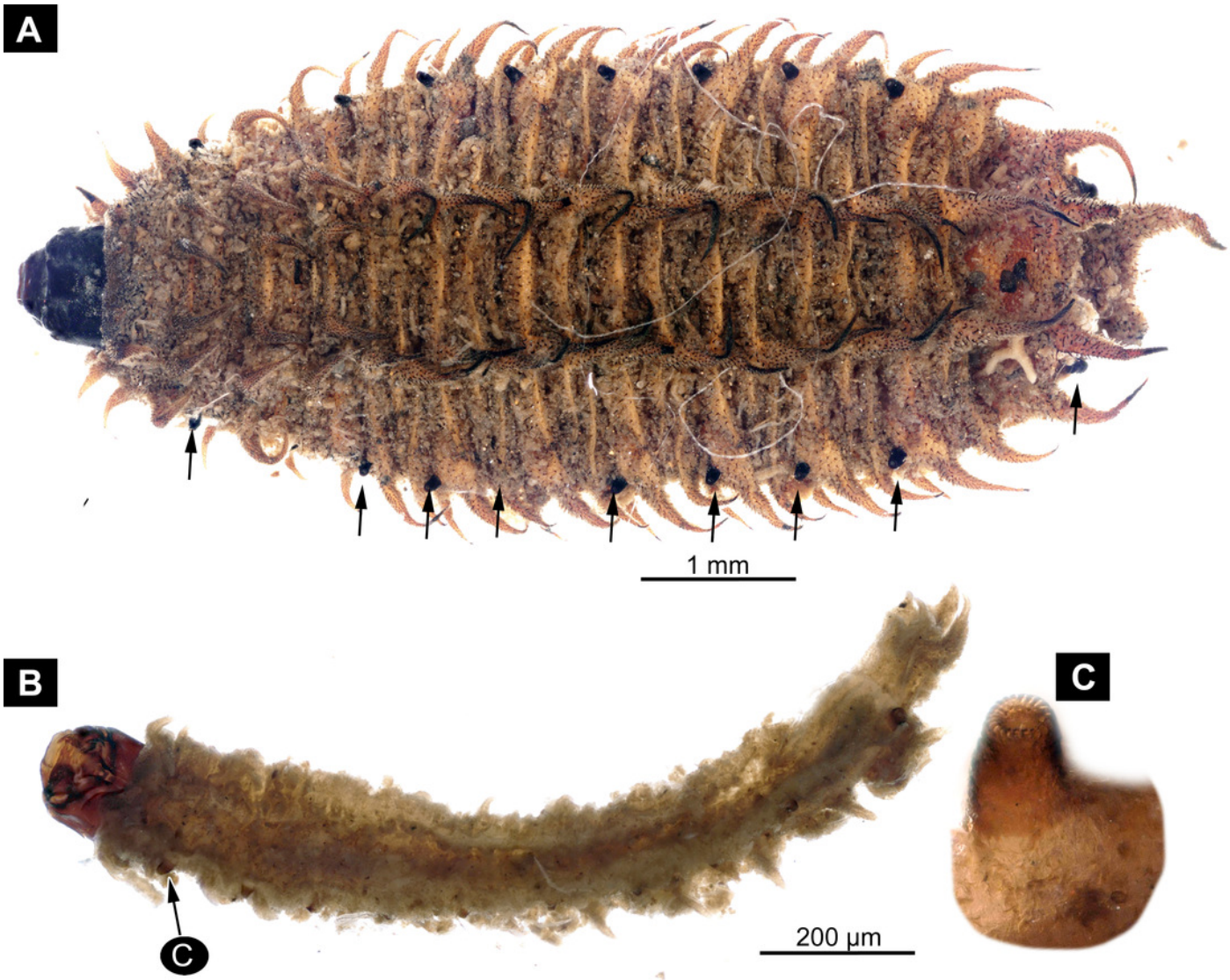

Figure 6

Fossil dipteran larva, *Pachyneura*, collection of GPIH, accession number (L-7617).

(A) habitus, dorsal. (B) schematic drawing of habitus, dorsal. a2–a8, abdominal segment 2–8; cl, clypeus; Abbreviations: hc, headcapsule; ms, mesothorax; mt, metathorax; pt, prothorax; s1–s10, spiracle 1–10.

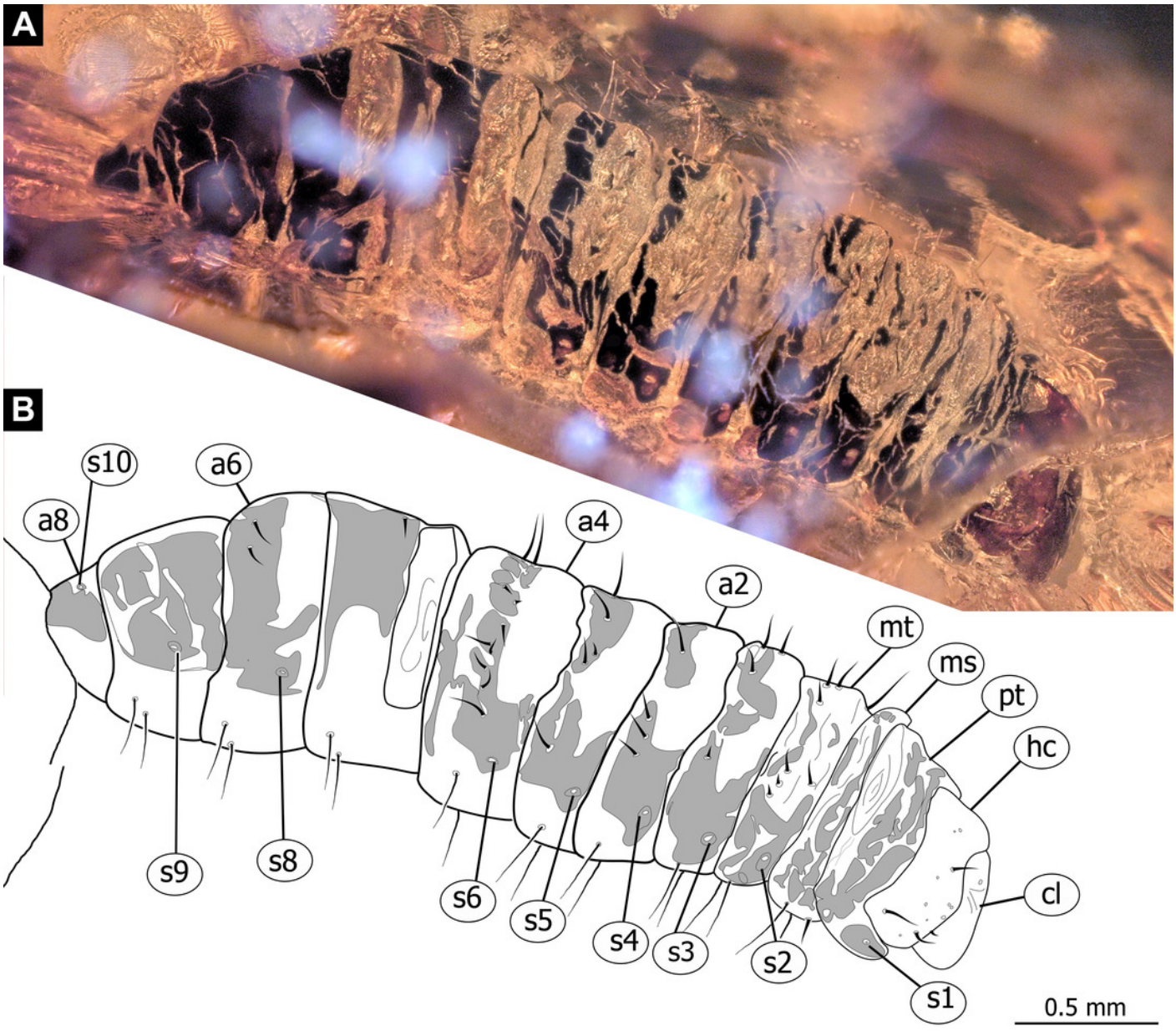

Figure 7

Fossil dipteran larva, *Pachyneura*, collection of GPIH (L-7617).

(A) habitus, ventral. (B) coloured version of A. Abbreviations: a1–a8, abdominal segments 1–8; c1–c6, creeping welts 1–6; hc, headcapsule; lb, labrum; md, mandibles; mp, maxillar palp; ms, mesothorax; mt, metathorax; mx, maxilla; pt, prothorax; te, trunk-end.

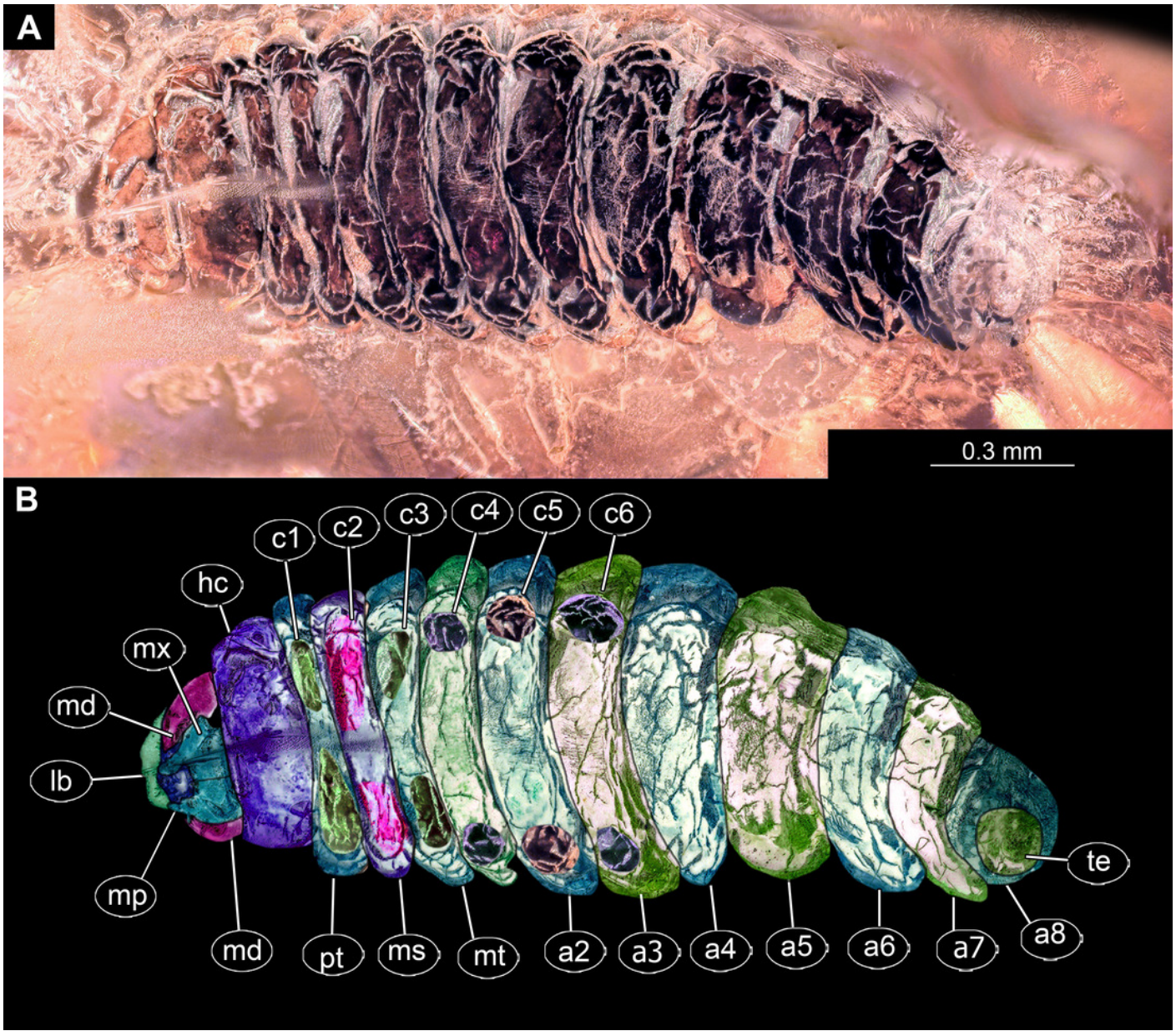

Figure 8

Fossil dipteran larva, *Pachyneura*, collection of GPIH, accession number (L-7617).

(A) head capsule, dorsal view. (B) head capsule, ventral view. (C) coloured version of B. (D) head capsule ventral view, schematic drawing. Abbreviations: hb, hypostomal bridge; hc, head capsule; lb, labrum; md, mandibles; mp, maxilary palps; mx, maxillae.

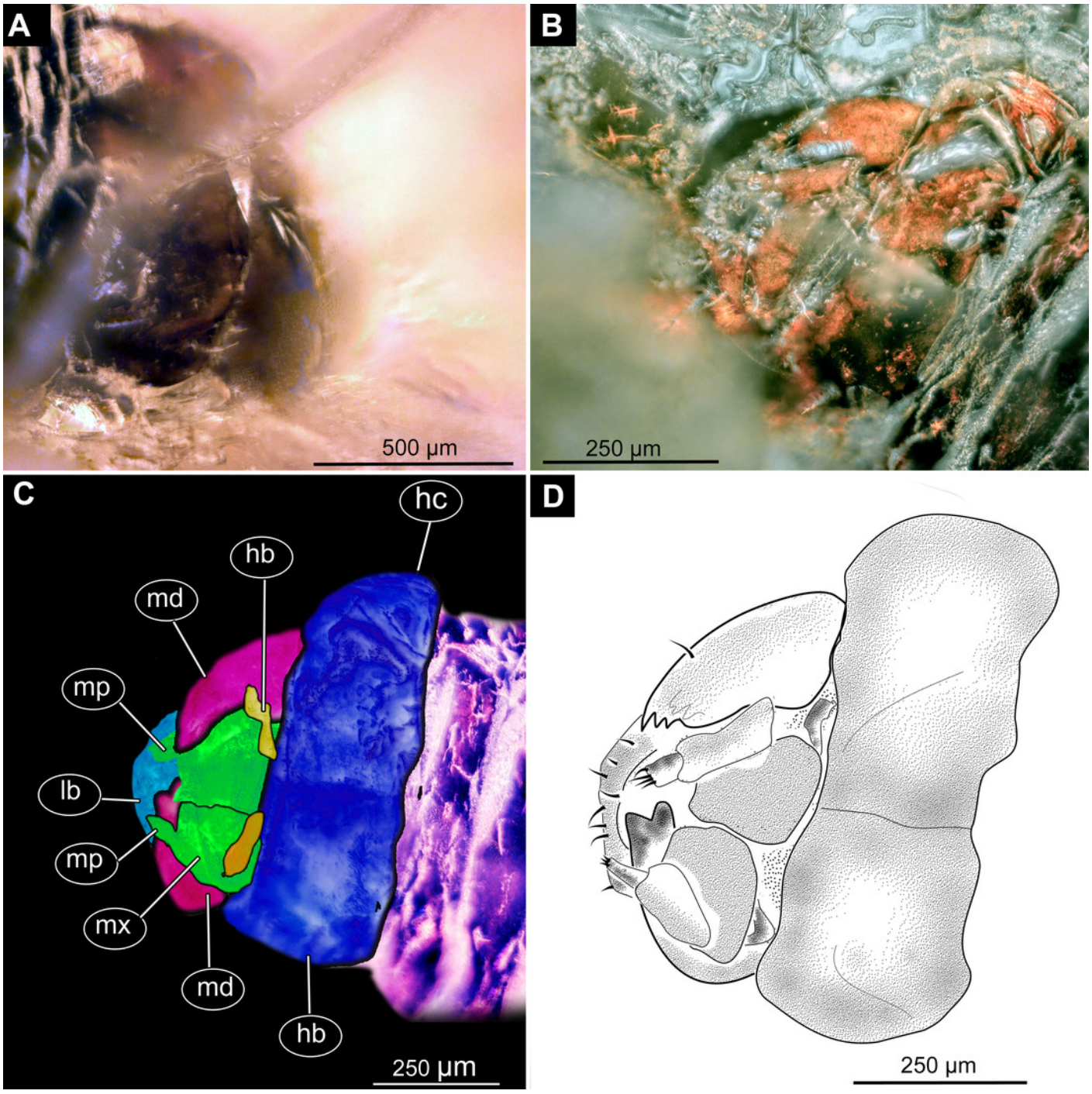
A
500 µm
B
250 µm
C
hc
hb
md
mp
lb
mp
mx
md
hb
250 µm
D
250 µm

Figure 9

Fossil dipteran larva, *Mycetobia*, DEI, accession number Dip-00640.

(A) habitus, dorsal view. (B) coloured version of A. (C) posterior spiracles, specimen 2 of B. (D) coloured version of C. Abbreviations: a2–a8, abdominal segments 2–8; as, anterior spiracle; hc, head capsule; ms, mesothorax; mt, metathorax; ps, posterior spiracle; pt, prothorax.

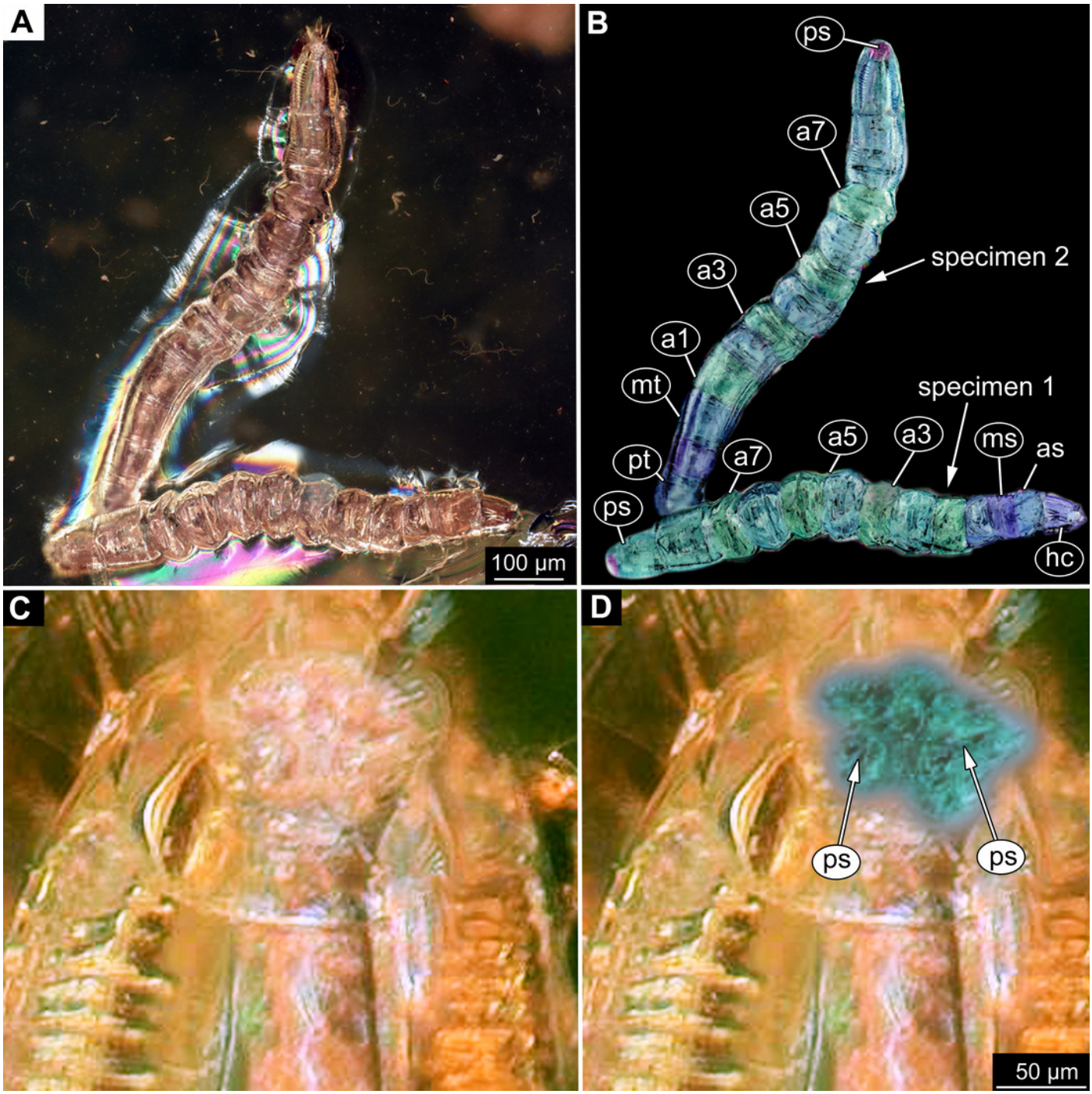
A
100 µm
B
ps
a7
a5
specimen 2
a3
a1
mt
specimen 1
pt
a7
a5
a3
ms
as
ps
hc
C
D
ps
ps
50 µm

Figure 10

Fossil dipteran larva, *Mycetobia*, DEI accession number Dip-00640, specimen 1 of Fig. 8B.

(A) head capsule, dorsal view. (B) anterior spiracle. (C) coloured version of A. (D) head capsule, ventral view. (E) coloured version of D. Abbreviations: an, antenna; as, anterior spiracle; hc, head capsule; lb, labrum; md, mandibles; mn, mentum; mp, maxilar palps; mx, maxillae; ps, posterior spiracle.

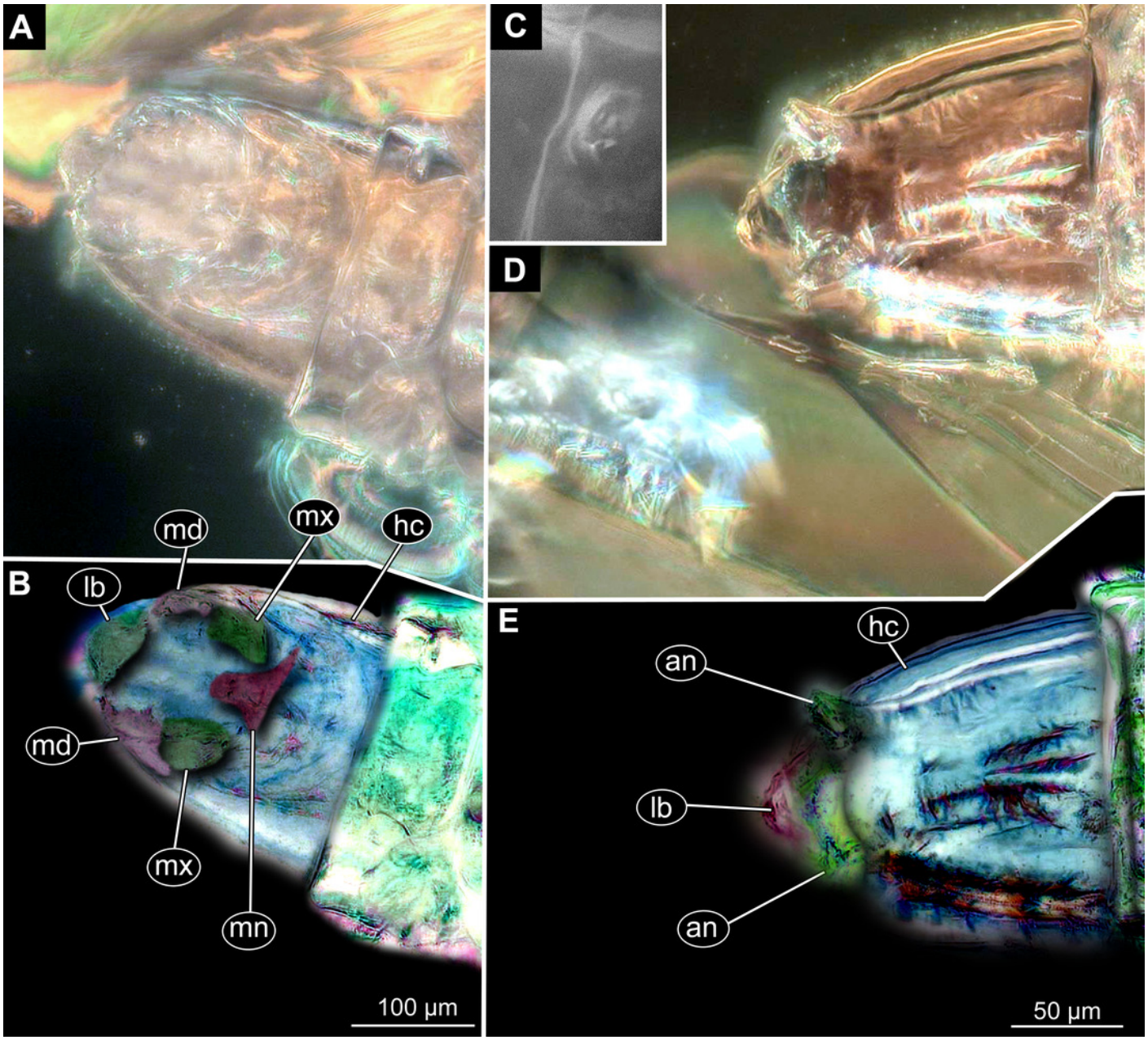
A
C
D
md
mx
hc
B
lb
md
mx
mn
100 µm
E
hc
an
lb
an
50 µm

Figure 11

Extant dipteran larva, *Mycetobia pallipes* Meigen, 1818, ZSM, no collection number assigned.

(A) habitus, lateral. (B) coloured version of A. (C) head capsule, lateral view. (D) coloured version of C. Abbreviations: a2–a8, abdominal segment 2–8; as, anterior spiracle; hc, head capsule; md, mandible; mn, mentum; ms, mesothorax; mt, methathorax; mx, maxillae; pt, prothorax; tp, posterior pit of tentorium.

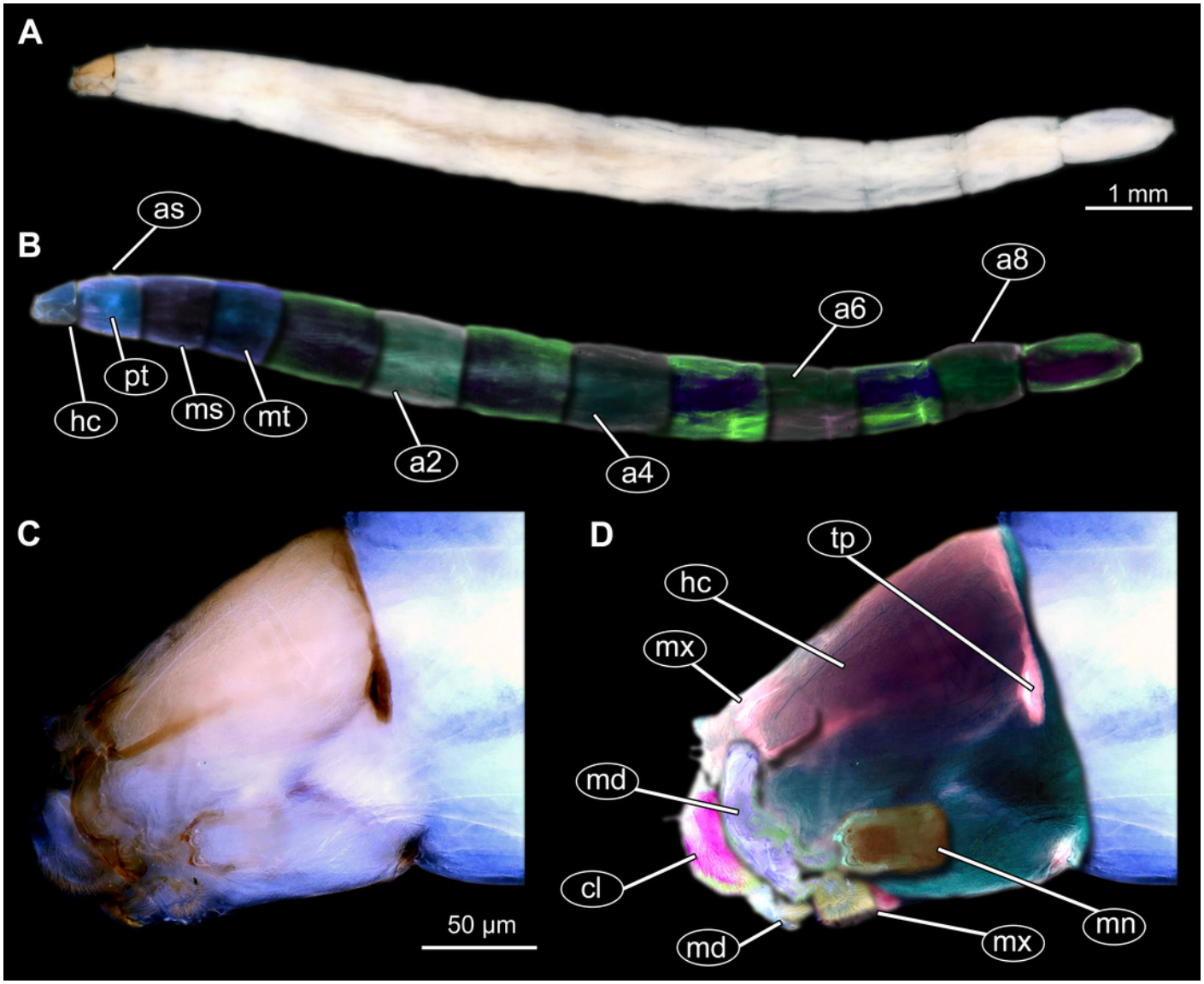

Figure 12

Fossil pupa, *Mycetobia connexa* (Mycetobia “morphotype 1”), GPIH, collection number 1851-DN.

(A) habitus, ventro-lateral view. (B) coloured version of A. Abbreviations: a3–a7, abdominal segments 3–7; an, antennae; fs, frontal setae; p1, front legs; p2, midlegs; p3, hind legs; te, trunk-end; wn, wings.

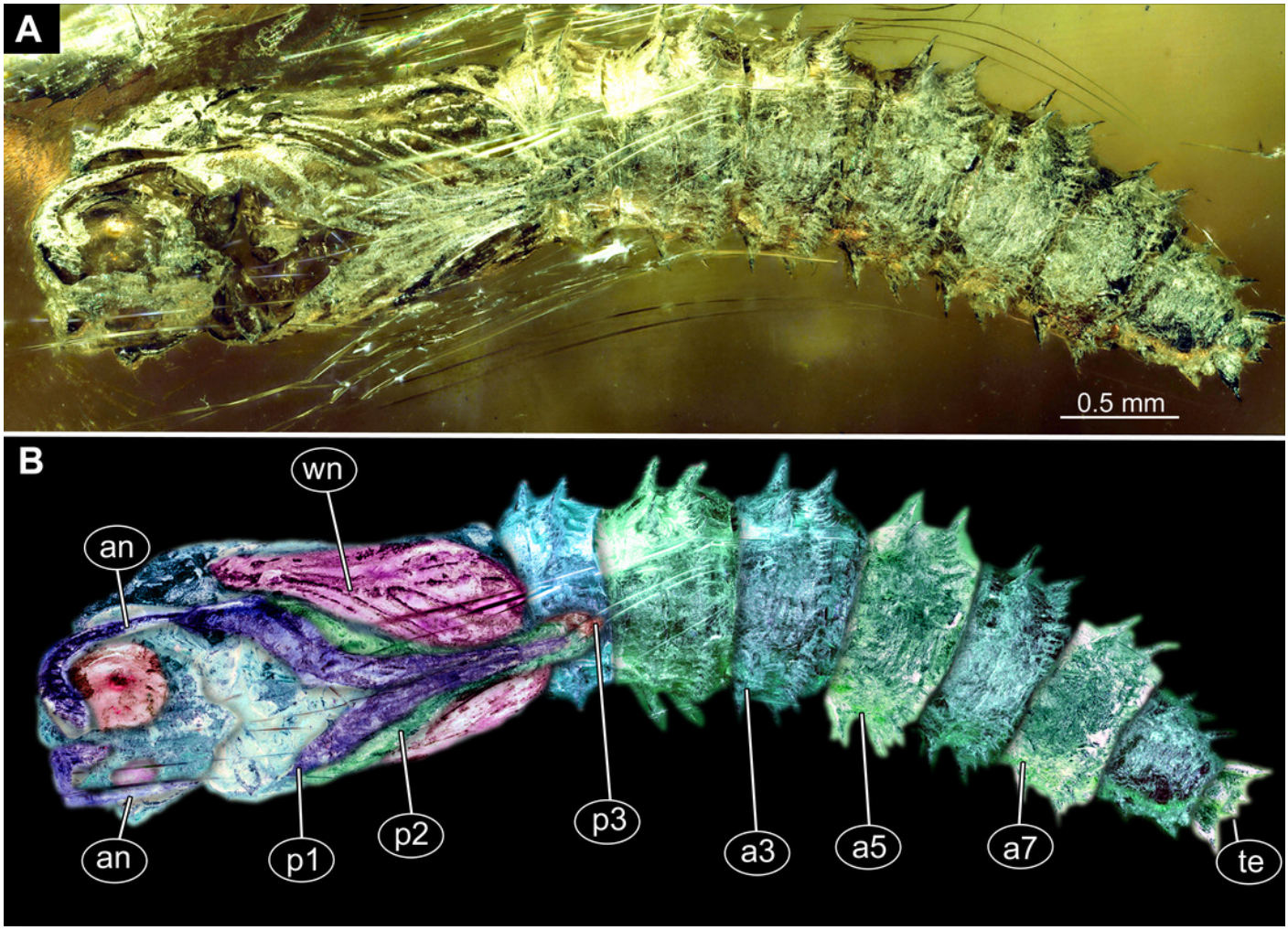

Figure 13

Fossil pupa, *Mycetobia* “morphotype 2”, PED, collection number PED-4866.

(A) habitus, lateral view. (B) coloured version of A. Abbreviations: a1–a8, abdominal segments 1–8; an, antennae; ey, eyes; ms, mesothorax; mt, metathorax; p1, front legs; p2, midlegs; p, prothorax; te, trunk-end; th, thoracic horns; wn, wings.

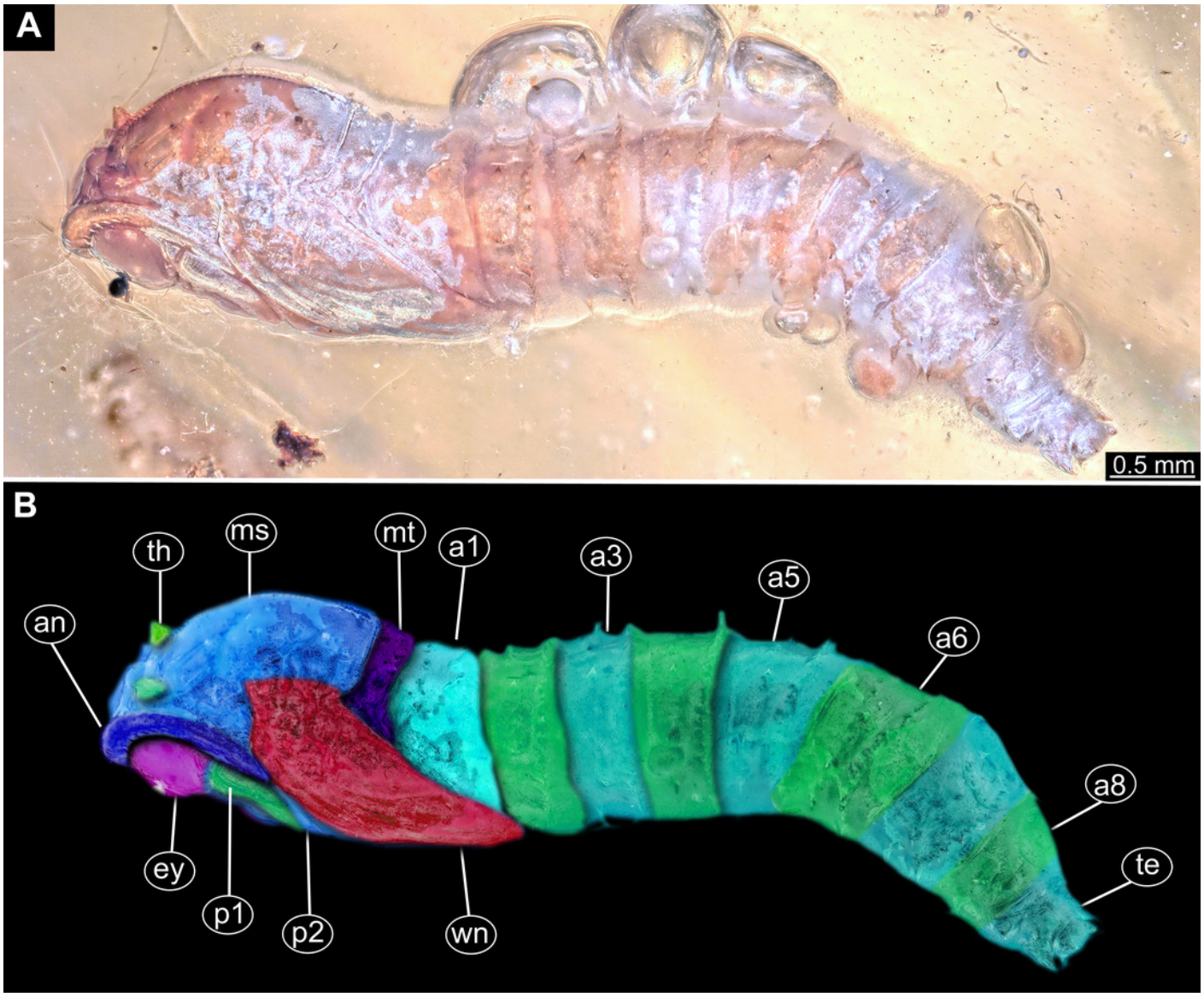

Figure 14

Fossil pupa, *Mycetobia* “morphotype 3”, pharate adult, DEI, collection number CCHH-DEI-608-2.

(A) habitus, dorsal view. (B) habitus, ventral view.

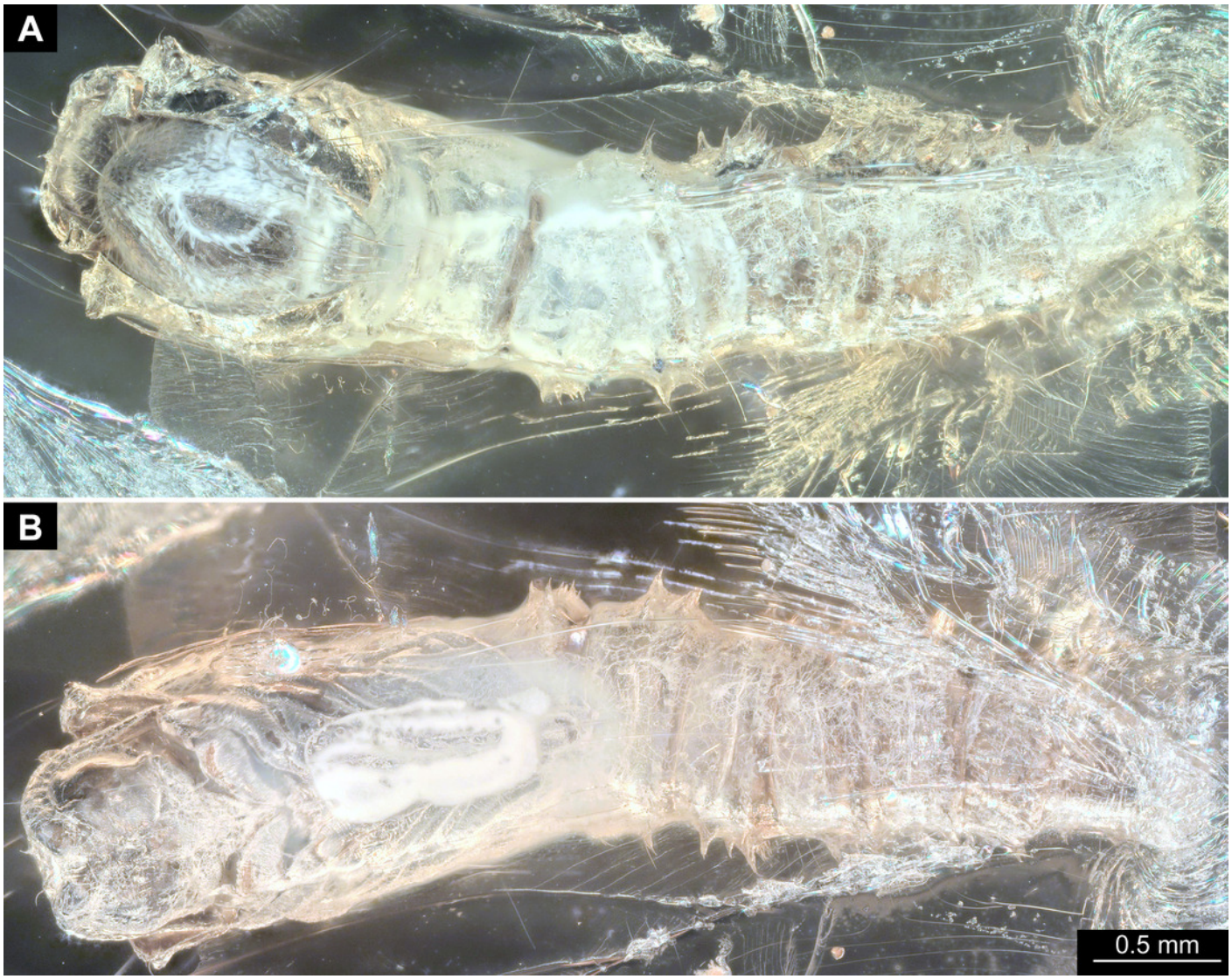

Figure 15

Extant pupa, *Mycetobia pallipes* Meigen, 1818, ZSM, no collection number assigned

(A) habitus, dorsal view. (B) coloured version of A. (C) habitus, ventral view. (D) coloured version of C. Abbreviations: an-antennae; a3–a7, abdominal segments 3–7: ey, eyes; fs, frontal setae; mt, mesothorax; p1, front legs; p2, midlegs; p3, hind legs; te, trunk-end; th, thoracic horn; wn, wing.

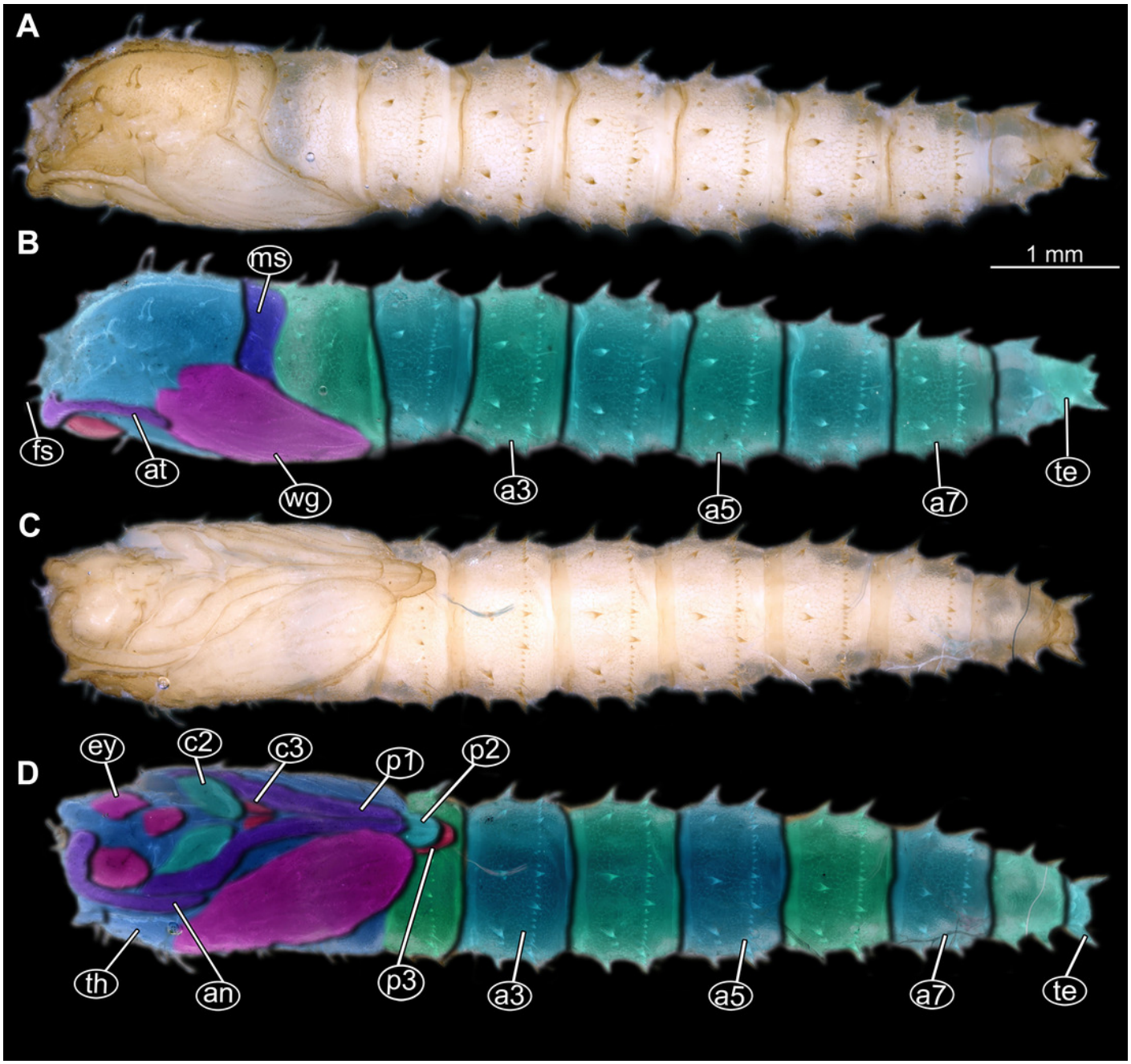
A
B
ms
1 mm
fs
at
wg
a3
a5
a7
te
C
D
ey
c2
c3
p1
p2
th
an
p3
a3
a5
a7
te

Figure 16

Fossil larva, *Sylvicola*, DEI, collection number Dip-00642.

(A) habitus, lateral view. (B) coloured version of A. (C) head capsule, lateral view. (D) coloured version of C. Abbreviations: a1–a8, abdominal segments 1–8; an, antennae; as, anterior spiracle; hc, head capsule; lb, labrum; md, mandible, mn, mentum; mx, maxilla; ms, mesothorax; te, trunk end.

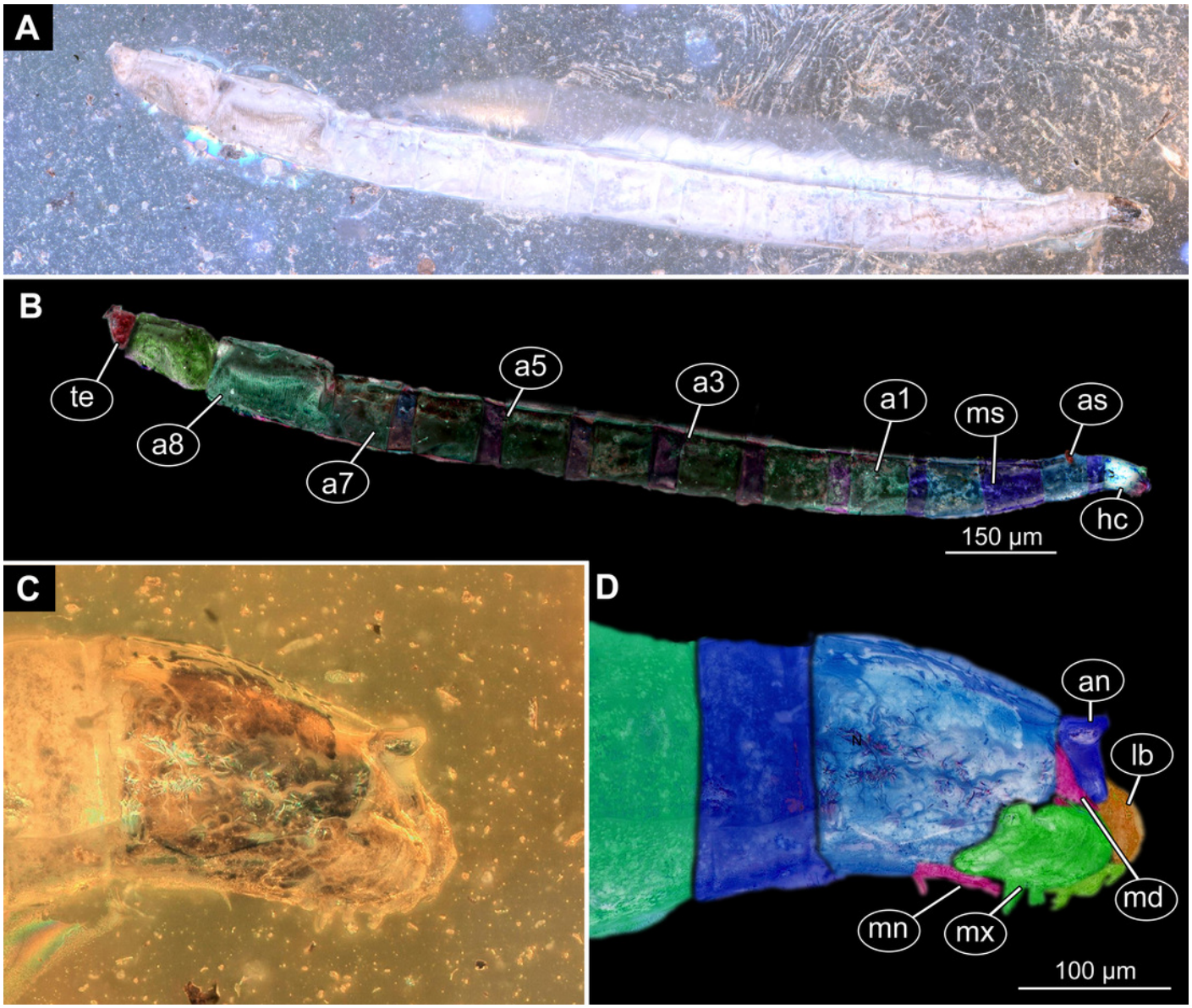

Figure 17

Reconstructed ontogenetic sequence for representatives of *Mycetobia* in the Eocene.

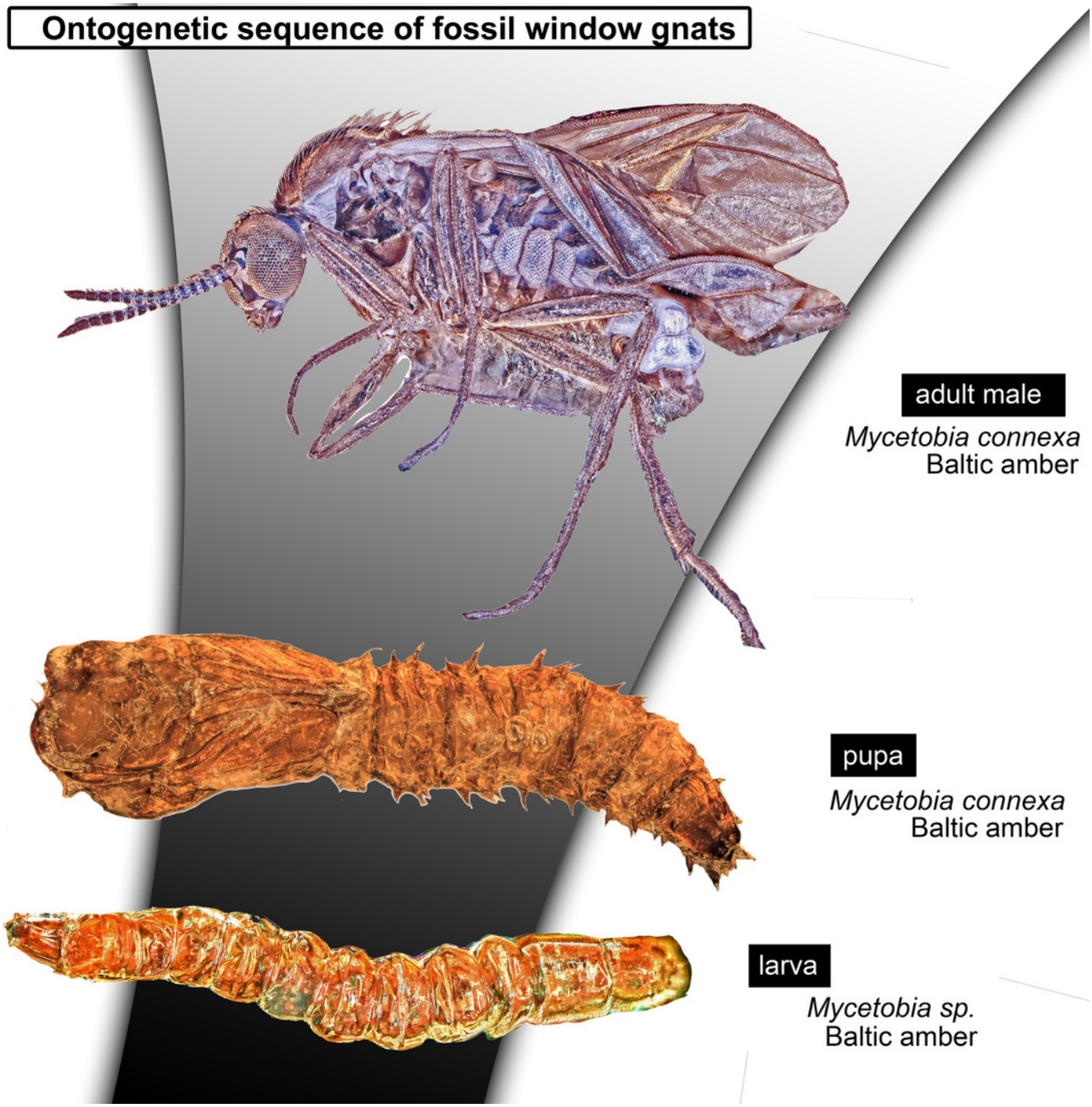

Figure 18

Summary statistics.

(A) biplot of fossil larvae of *Mycetobia* (n=36), head capsule length vs. head capsule width, red circles indicate hypothetical divisions into different larval stages based on the gaps in the data point distribution. I–IV, number of hypothetical larval stages. (B) distribution of the size cohorts within a sample of the fossil larvae of *Mycetobia*; upper-row-left, histogram of the head capsule width distribution (n=26); upper-row-center, histogram of the head capsule length distribution (n=25); upper-row-right, histogram of the body length distribution (n=36); lower-row-left, ranged plot (values ordered in ascending order) of the head capsule width, hypothetical division into different larval stages based on gaps in data point distribution indicated with I–IV as numbers of supposed larval stages; lower-row-centered, ranged plot (values ordered in ascending order) of head capsule length; lower-row-right, ranged plot (values ordered in ascending order) of body length.

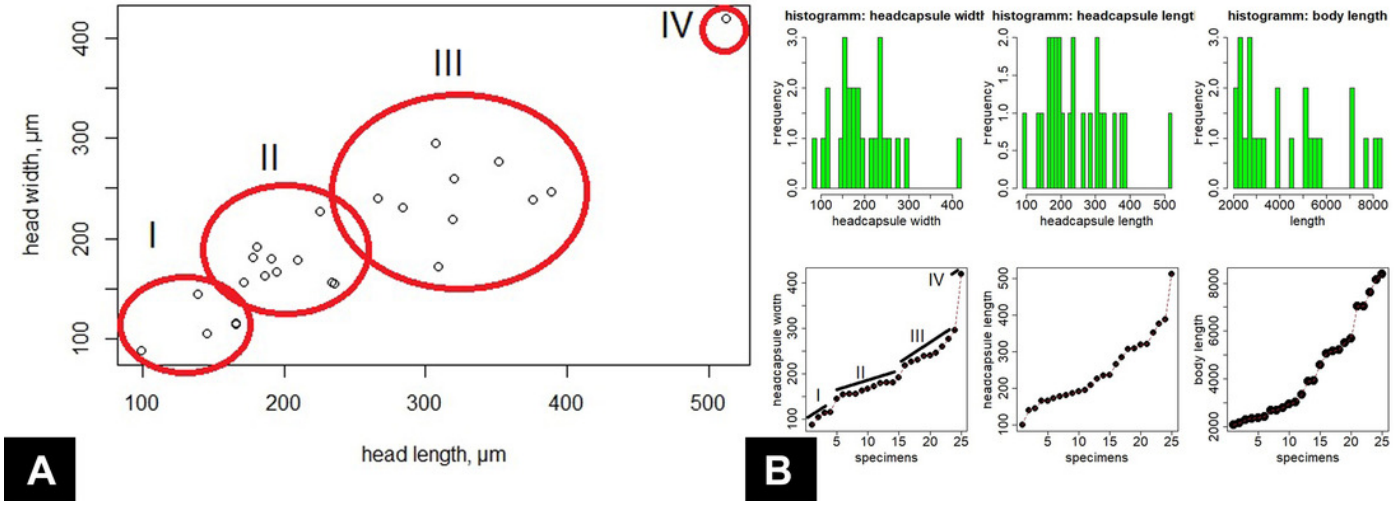

Figure 19

Natural logarithm of the mean larval head capsule width and head capsule of fossil larvae of *Mycetobia*, plotted against associated instar number.